

Social stress induces neurovascular pathology promoting depression

Caroline Menard^{1,8}, Madeline L. Pfau¹, Georgia E. Hodes¹, Veronika Kana², Victoria X. Wang³, Sylvain Bouchard¹, Aki Takahashi^{1,4}, Meghan E. Flanigan¹, Hossein Aleyasin¹, Katherine B. LeClair¹, William G. Janssen¹, Benoit Labonté¹, Eric M. Parise¹, Zachary S. Lorsch¹, Sam A. Golden¹, Mitra Heshmati¹, Carol Tamminga⁵, Gustavo Turecki⁶, Matthew Campbell⁷, Zahi A. Fayad³, Cheuk Ying Tang³, Miriam Merad² and Scott J. Russo^{1*}

Studies suggest that heightened peripheral inflammation contributes to the pathogenesis of major depressive disorder. We investigated the effect of chronic social defeat stress, a mouse model of depression, on blood–brain barrier (BBB) permeability and infiltration of peripheral immune signals. We found reduced expression of the endothelial cell tight junction protein claudin-5 (Cldn5) and abnormal blood vessel morphology in nucleus accumbens (NAc) of stress-susceptible but not resilient mice. *CLDN5* expression was also decreased in NAc of depressed patients. *Cldn5* downregulation was sufficient to induce depression-like behaviors following subthreshold social stress whereas chronic antidepressant treatment rescued *Cldn5* loss and promoted resilience. Reduced BBB integrity in NAc of stress-susceptible or mice injected with adeno-associated virus expressing shRNA against *Cldn5* caused infiltration of the peripheral cytokine interleukin-6 (IL-6) into brain parenchyma and subsequent expression of depression-like behaviors. These findings suggest that chronic social stress alters BBB integrity through loss of tight junction protein *Cldn5*, promoting peripheral IL-6 passage across the BBB and depression.

Major depressive disorder (MDD) is the leading cause of worldwide disability and the most prevalent mood disorder^{1,2}. The prevalence of MDD is two- to threefold higher in patients with cardiovascular disease and, conversely, MDD is associated with an ~80% increased risk of cardiovascular morbidity and mortality^{1,3–5}. Chronic inflammation and sustained increases in circulating pro-inflammatory cytokines have been associated with atherosclerotic plaque formation, progression and rupture, likely contributing to the pathogenesis of cardiovascular disease and heart failure⁶. Concomitantly, clinical studies report higher levels of circulating pro-inflammatory cytokines in patients with MDD, a pattern that has been replicated in preclinical animal models of depression^{1,7–10}. Individual differences in the peripheral immune system and modulation of cytokine release, notably IL-6, are associated with susceptibility versus resilience to chronic social stress¹¹. Chronic stress mobilizes the innate immune system and stimulates enhanced proliferation and release of inflammatory monocytes and neutrophils into the bloodstream^{12,13}.

It has been hypothesized that peripheral myeloid cells or pro-inflammatory cytokines can diffuse into the brain of stressed individuals as a result of stress-induced neurovascular damage and increased BBB permeability^{7,14–19}. Indeed, a clinical study reported an altered cerebrospinal fluid to serum ratio of peripheral markers in depressed patients, suggesting that BBB integrity is compromised²⁰. However, the possible link between BBB permeability, stress vulnerability and depression is still controversial²¹. The BBB is formed by endothelial cells sealed by tight junction proteins,

pericytes and astrocytes, and serves to prevent potentially harmful signals in the blood from entering the brain. Here we evaluate the effect of chronic social defeat stress (CSDS), a mouse model of depression, on BBB-related gene expression and define a role for the tight junction protein claudin 5 (*Cldn5*) in the establishment of depression-like behaviors and MDD. *Cldn5* is a major cell adhesion molecule in endothelial cells²², and loss of *Cldn5* has been shown to promote loosening of the BBB and increased permeability²³. Our study thus characterizes and functionally interrogates the neurovascular pathology associated with social stress vulnerability.

Results

Vulnerability to chronic social stress and MDD are associated with loss of tight junction protein *Cldn5* expression. Chronic social stress is a prominent contributor to mood disorder prevalence and suicide attempts in victims of bullying²⁴. Similarly, in rodents, CSDS induces a depression-like phenotype (social avoidance, anhedonia) in a subset of mice, termed stress-susceptible (SS), that can be reversed by chronic, but not acute, antidepressant treatment^{25,26}. In the CSDS protocol, a male C57BL/6J mouse is exposed daily (10 min/d) to bouts of social defeat by a larger, physically aggressive CD-1 mouse²⁷ (Fig. 1a). Defeated mice that do not display social avoidance as assessed with the social interaction (SI) test (Supplementary Fig. 1a–c) are considered resilient (RES). We compared SS to RES mice to identify individual differences in the neurovascular mechanisms potentially underlying chronic stress responses. First, we performed transcriptional profiling of

¹Fishberg Department of Neuroscience and the Friedman Brain Institute, Icahn School of Medicine at Mount Sinai, New York, NY, USA. ²Department of Oncological Sciences, Tisch Cancer Institute and Immunology Institute, Icahn School of Medicine at Mount Sinai, New York, NY, USA. ³Department of Radiology, Translational and Molecular Imaging Institute at Mount Sinai, New York, NY, USA. ⁴University of Tsukuba, Tsukuba, Japan. ⁵Department of Psychiatry, University of Texas Southwestern Medical Center, Dallas, TX, USA. ⁶Douglas Mental Health University Institute and McGill University, Montreal, QC, Canada. ⁷Smurfit Institute of Genetics, Trinity College Dublin, Dublin 2, Ireland. Present address: ⁸Département de psychiatrie et neurosciences, Faculté de médecine and CERVO Brain Research Centre, Université Laval, Quebec City, QC, Canada. *e-mail: scott.russo@mssm.edu

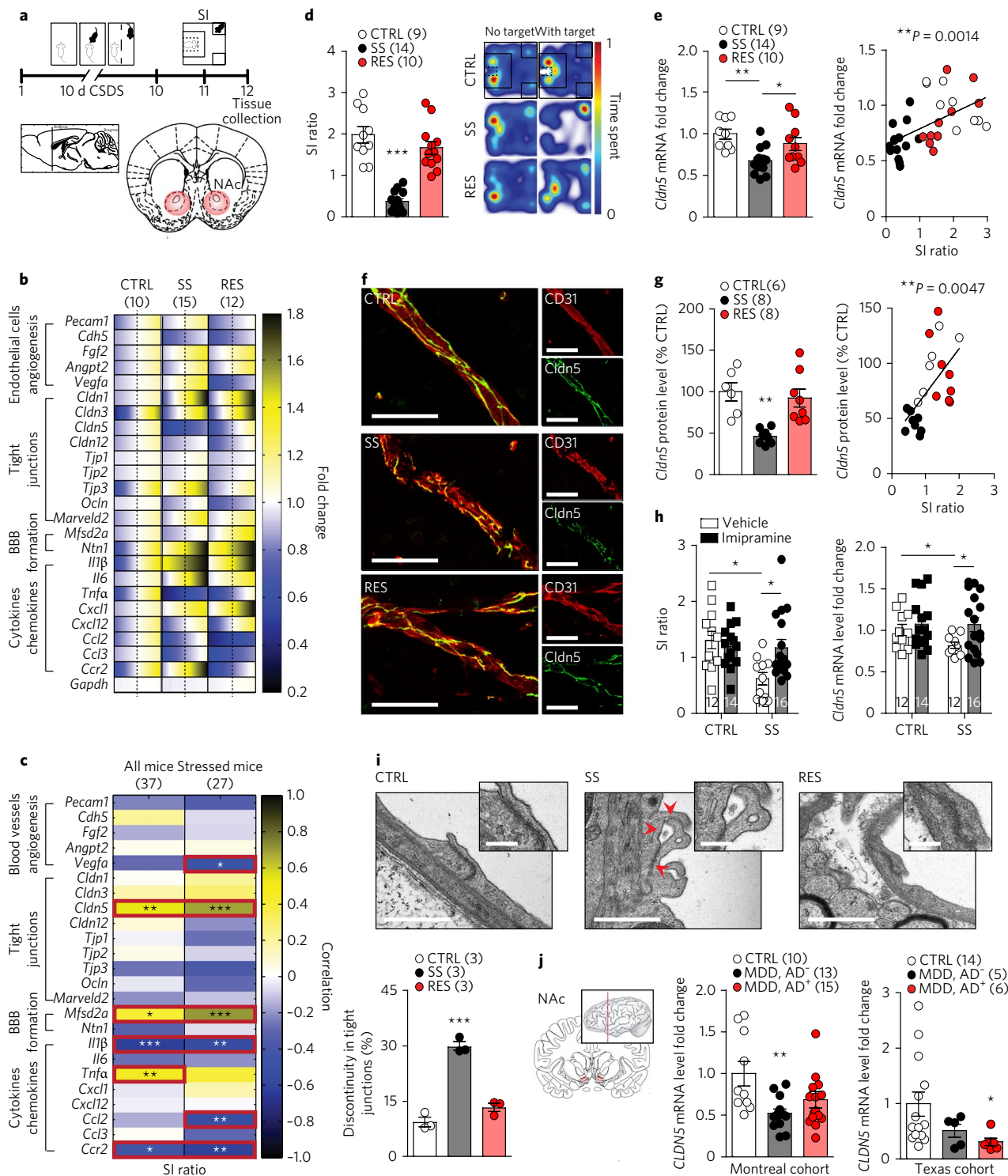


Fig. 1 | Social stress vulnerability and MDD is associated with reduced *Cldn5* expression. **a**, Experimental timeline of 10-d chronic social defeat stress (CSDS), social interaction (SI) behavioral screening and tissue collection of NAc. **b**, Quantitative PCR revealed significant changes in the NAc of stress-susceptible (SS) and resilient (RES) mice when compared to unstressed controls (CTRL) for gene expression related to endothelial cell biology, angiogenesis, tight junctions, BBB formation, cytokines and chemokines. The range of color indicates individual differences within a group; s.e.m. from the average represented by the dashed line. **c**, Several patterns of gene expression correlated with SI ratio. **d**, Individual SI ratio values (left) and representative heat maps of normalized time spent during SI test are shown on the right. **e–g**, *Cldn5* mRNA (**e**) and *Cldn5* protein (**f,g**) levels were lower in the NAc of SS mice and correlated with social avoidance. Scale bars, 20 μ m. **h**, Chronic treatment with imipramine reversed social avoidance and rescued *Cldn5* loss in SS mice. **i**, Transmission electron microscopy revealed discontinuities (red arrows) in tight junctions of SS but not resilient mice. Scale bars, 500 nm (250 nm for insets); 52–66 tight junctions per mouse and 3 mice per group. **j**, *CLDN5* mRNA level fold change was significantly lower in the NAc of MDD patients from two different cohorts. AD, antidepressant. Data represent mean \pm s.e.m.; number of animals or subjects (*n*) is indicated on graphs. Two-way ANOVA followed by Bonferroni’s multiple comparison test for antidepressant treatment; correlations were evaluated with Pearson’s correlation coefficient; one-way ANOVA followed by Bonferroni’s multiple comparison test for other graphs, **P* < 0.05; ***P* < 0.01; ****P* < 0.001.

BBB-related and cytokine and chemokine gene expression in the nucleus accumbens (NAc) of unstressed control (CTRL), SS and RES mice after 10-d CSDS (Fig. 1b; quantitative PCR primers are listed in Supplementary Table 1). The NAc plays a crucial role in stress responses and mood disorders, including MDD²⁸. CSDS induced changes in the expression of genes involved in endothelial cell biology, angiogenesis, vascular permeability, and BBB formation and function (Fig. 1b). Notably, *Cldn5* mRNA was significantly reduced in NAc of SS mice compared to CTRL and RES mice, and levels positively correlated with social avoidance behavior ($P=0.0014$) (Fig. 1c–e). Normalization of *Cldn5* and other tight junction mRNA expression to platelet endothelial cell adhesion molecule (*Pecam1*), an endothelial cell marker also known as cluster of differentiation 31 (CD31), confirmed ~40% loss of *Cldn5* expression in SS mice ($P=0.0009$) (Supplementary Fig. 1d,e). *Cldn5* is an endothelial-cell-specific tight junction protein (Supplementary Fig. 2d)^{29,30}, which we confirmed to be enriched in blood vessels using a brain capillary extraction method (Supplementary Fig. 2e). We next detected a specific reduction of *Cldn5* protein in SS mice by examining its colocalization with CD31 (Fig. 1f). *Cldn5* protein levels in NAc blood vessels also positively correlated with social avoidance behavior ($P=0.0047$) (Fig. 1g and Supplementary Fig. 2a–c). No difference was observed for CD31 or other tight junction proteins in the NAc (Supplementary Fig. 2f).

We next evaluated whether significant changes in *Cldn5* expression were present after CSDS in other brain regions that contribute to depression symptomatology²⁸. *Cldn5* mRNA levels in the hippocampus of both SS and RES mice were significantly lower than in unstressed CTRL mice ($P=0.0024$) (Supplementary Fig. 1f). However, *Cldn5* and occludin protein levels were significantly higher in the hippocampus of RES mice when compared to SS but not CTRL mice, suggesting compensatory mechanisms in this brain region (Supplementary Fig. 3a). No difference was observed between SS, RES and CTRL mice in the prefrontal cortex (PFC) or hypothalamus (Supplementary Figs. 1g,h and 3b). We next used transmission electron microscopy to show that CSDS induces ultrastructural abnormalities of blood vessels within the NAc of SS, but not RES, mice (Fig. 1i and Supplementary Fig. 4a–c). In SS mice, blood vessels were characterized by discontinuous tight junctions ($P<0.0001$) (Fig. 1i). Ultrastructural abnormalities were present in both large vessels and capillaries of the NAc (Supplementary Fig. 4d). No significant change was observed in the PFC of SS or RES mice when compared to unstressed CTRL mice (Supplementary Fig. 4e).

Additionally, we evaluated the effect of nonsocial chronic stressors on *Cldn5* expression in the NAc. Male C57BL/6J mice subjected to 28 d of chronic variable stress, which also induces a depression-like phenotype, displayed reduced *Cldn5* mRNA expression in the NAc ($P=0.0089$) (Supplementary Fig. 1j). However, no change was observed after 6 d of variable stress (subchronic variable stress), a protocol that is insufficient to induce depression-like behaviors in male mice³¹ (Supplementary Fig. 1i). These findings suggest that stress-induced reduction of *Cldn5* expression occurs in multiple brain regions in response to both social and nonsocial stress; however, *Cldn5* downregulation by stress does not occur ubiquitously throughout the brain and therefore is likely to play a specialized role in depression-like symptomatology.

Chronic antidepressant treatment can reverse CSDS-induced depression-like behaviors, including social avoidance^{25,32}. Thus, we evaluated the effect of chronic imipramine treatment on *Cldn5* expression in the NAc of SS mice. Following CSDS and behavioral phenotyping by SI, SS mice were treated with either vehicle or imipramine via intraperitoneal (i.p.) injection (20 mg per kilogram of body weight) for 35 d alongside unstressed vehicle or imipramine control groups (Supplementary Fig. 5a). As expected, social avoidance was rescued in the imipramine-treated but not vehicle-treated group (interaction treatment \times stress: $P=0.0201$) (Fig. 1h and

Supplementary Fig. 5b–d). Chronic imipramine treatment also normalized *Cldn5* mRNA expression in the NAc of SS mice (Fig. 1h) whereas acute imipramine injection was not sufficient to alter *Cldn5* mRNA (Supplementary Fig. 5e) or social avoidance³². Finally, we evaluated *CLDN5* mRNA expression in post-mortem NAc tissue from subjects with MDD. We used samples from two independently collected MDD cohorts, one from McGill University (Montreal cohort) and a second from the University of Texas Southwestern Medical Center (Texas cohort). About half of the MDD subjects in each cohort were on medication at time of death as determined by toxicology reports (Supplementary Tables 2 and 3). *CLDN5* mRNA expression was significantly reduced in the NAc of unmedicated MDD patients when compared to healthy controls in the Montreal cohort ($P=0.0117$), and this effect was only partially rescued by medication (Fig. 1j and Supplementary Fig. 5f). In the Texas cohort, *CLDN5* mRNA level was significantly reduced between MDD patients and healthy controls ($P=0.0435$), with no effect of medication (Fig. 1j and Supplementary Fig. 5f). No significant difference was observed for hippocampus and PFC when compared to healthy subjects (Supplementary Fig. 5g). Lack of significant medication effects may be related to suicide as cause of death for the majority of MDD patients in our cohorts. In addition, loss of *CLDN5* may be at least partly specific to mood disorders as no change was observed in post-mortem NAc tissue from cocaine users when compared to healthy controls (Supplementary Fig. 5h).

Downregulation of *Cldn5* expression induces depression-like behaviors.

To confirm a causal role for *Cldn5* downregulation in social-stress-induced depression-like behaviors, we conducted functional studies using virally mediated conditional knockdown of *Cldn5* in the NAc. We chose this conditional approach because *Cldn5*-deficient mice die within 10h of birth³³ and social stress testing needed to be conducted in adult mice. Stress-naive adult male mice received stereotactic intra-NAc injections of adeno-associated virus (AAV-2/9 serotype) expressing a doxycycline-inducible, *Cldn5*-targeting shRNA transcript (AAV-shRNA-*Cldn5*) or a control nontargeting vector (AAV-shRNA)³³. We confirmed that injection of AAV-shRNA-*Cldn5* virus into the NAc followed by treatment with doxycycline induced downregulation of *Cldn5* mRNA ($P=0.0016$) (Fig. 2b) and protein ($P=0.0013$) (Fig. 2c). No change was observed for other claudins or markers of endothelial cells, pericytes, astrocytes and microglia (Supplementary Fig. 6a; quantitative PCR primers are listed in Supplementary Table 4) or for protein level of endothelial cell marker CD31 (Supplementary Fig. 6b). For behavioral studies, mice were again injected with AAV-shRNA-*Cldn5* or AAV-shRNA and then allowed 2 weeks recovery before doxycycline treatment to induce expression of *Cldn5* shRNA. Half the mice were subjected to a subthreshold microdefeat consisting of three 5-min bouts of social defeat, each separated by a 15-min period of rest (Fig. 2a). Without the introduction of pro-depressive manipulations, this protocol is insufficient to induce depression-like behaviors and thus can be used to identify pro-susceptibility factors³². All AAV-injected mice were then subjected to a battery of depression- and anxiety-related behavioral tests (Fig. 2a). Loss of *Cldn5* did not affect baseline depression-like behaviors; however, when combined with subthreshold microdefeat, *Cldn5* downregulation induced depression-like behaviors across multiple behavioral assays. Stressed AAV-shRNA-*Cldn5* mice spent significantly less time grooming in the splash test ($P=0.0356$) (Fig. 2d), displayed anhedonia as assessed with the sucrose preference test ($P=0.0063$) (Fig. 2e) and spent more time immobile in the forced swim test ($P=0.0015$) (Fig. 2f). They also displayed greater social avoidance when compared to unstressed controls and stressed AAV-shRNA mice as measured by lower SI ratio, calculated by dividing the interaction zone time when social target is present by interaction zone time when the target is absent ($P=0.0386$) (Fig. 2g). Stressed

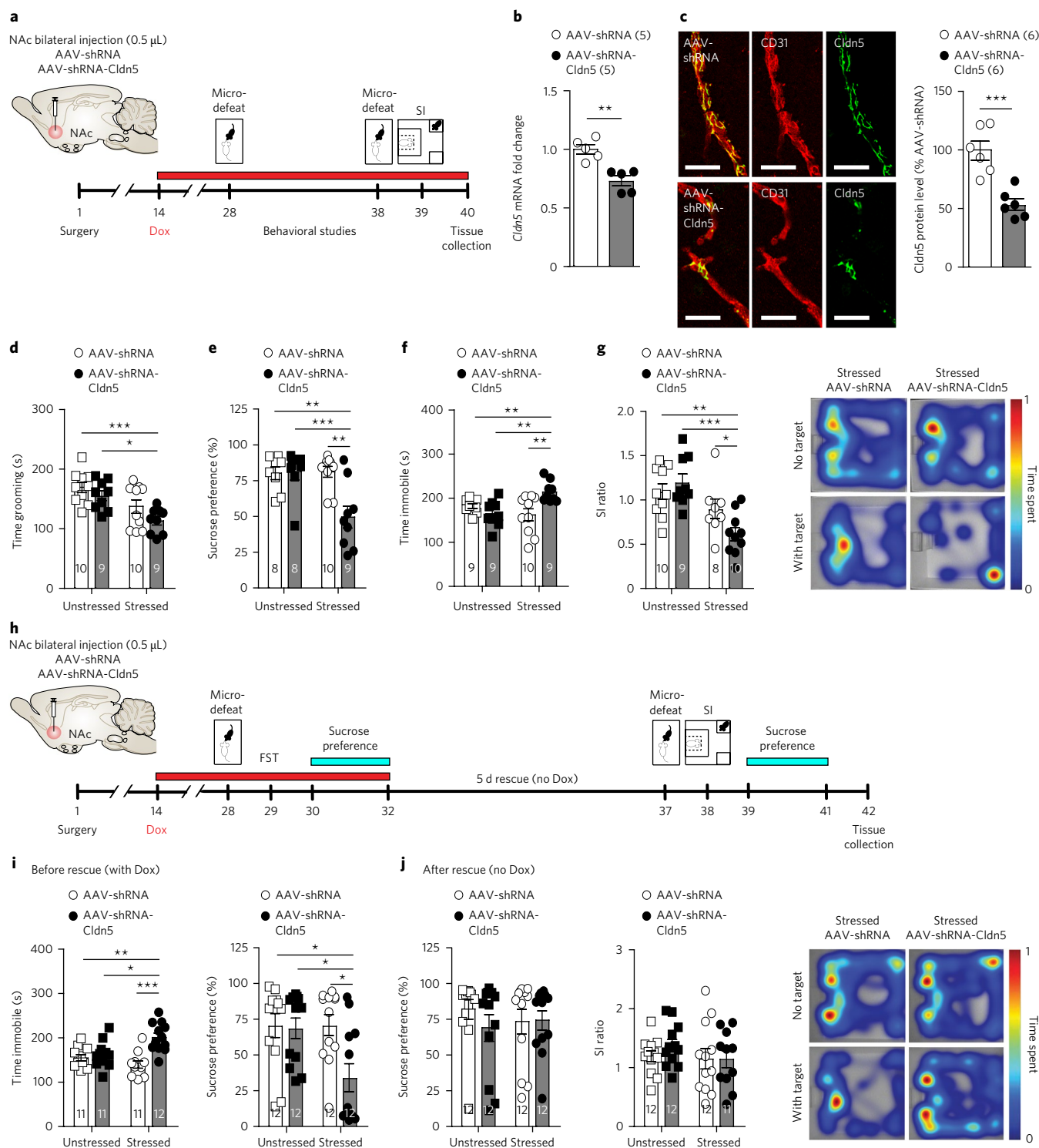


Fig. 2 | Conditional knockdown of *Cldn5* expression in the NAc is sufficient to induce depression-like behaviors. **a**, Experimental timeline of NAc bilateral injection of AAV-shRNA or AAV-shRNA-Cldn5 viruses and behavioral studies. **b,c**, *Cldn5* mRNA (**b**) and *Cldn5* protein (**c**) levels are reduced following AAV-shRNA-Cldn5 injection in the NAc of stress-naïve mice when compared to that in AAV-shRNA-injected animals. Co-staining with CD31 confirmed lower *Cldn5* protein level in blood vessels following AAV-shRNA-Cldn5 virus injection and doxycycline (Dox) treatment (**c**). Scale bars, 20 μ m. **d-g**, Downregulation of *Cldn5* expression before subthreshold microdefeat (stressed mice) induced depression-like behaviors as assessed by splash (**d**), sucrose preference (**e**), forced swim (**f**) and social interaction (**g**) tests. The effect was significant when compared to unstressed mice and stressed AAV-shRNA. **h**, Experimental timeline of *Cldn5* rescue experiment. **i**, Stressed AAV-shRNA-Cldn5 mice displayed depression-like behaviors when subjected to doxycycline treatment as assessed with forced swim test and sucrose preference. **j**, No difference was observed between groups for sucrose preference and social interaction when doxycycline was removed from the water, allowing normal *Cldn5* expression. Data represent mean \pm s.e.m.; number of animals (*n*) is indicated on graphs. Unpaired *t*-test for virus validation or two-way ANOVA followed by Bonferroni's multiple comparison test for behaviors, **P* < 0.05; ***P* < 0.01; ****P* < 0.001.

AAV-shRNA-Cldn5 mice also spent less time in the interaction zone ($P=0.0064$) and more time in the corners ($P=0.0463$) when the social target was present (Supplementary Fig. 6c) compared to unstressed controls and stressed AAV-shRNA mice. By contrast, AAV-shRNA-Cldn5 had no effect on anxiety-related behaviors as assessed with the novelty-suppressed feeding (Supplementary Fig. 6d), elevated plus maze (Supplementary Fig. 6e) and open field (Supplementary Fig. 6f) tests. Because we observed higher Cldn5 protein level in RES mice after 10-d CSDS when compared to SS mice (Supplementary Fig. 3a), we also evaluated the effect of virally mediated downregulation of *Cldn5* expression in this brain region. Injection of AAV-sRNA-Cldn5 and AAV-shRNA viruses in the hippocampus (Supplementary Fig. 7a,b) had no effect on grooming in the splash test or sucrose preference; however, stressed AAV-shRNA-Cldn5 mice displayed greater social avoidance ($P=0.0005$) (Supplementary Fig. 7c–f). Mice injected with AAV-shRNA-Cldn5 also spent more time immobile in the forced swim test (two-way ANOVA, virus effect $P=0.0396$) (Supplementary Fig. 7e), suggesting a region-specific effect for some, but not all, behaviors. Finally, we performed a rescue experiment to confirm the causal role of NAc *Cldn5* expression in the establishment of depression-like behaviors (Fig. 2h and Supplementary Fig. 7g). Two cohorts of mice were injected with either AAV-shRNA-Cldn5 or AAV-shRNA and allowed 2 weeks recovery before doxycycline treatment to induce expression of *Cldn5* shRNA. Half of the mice in each cohort were subjected to a subthreshold microdefeat, and establishment of depression-like behaviors was confirmed in stressed AAV-shRNA-Cldn5 mice with forced swim test and sucrose preference test (Fig. 2h,i and Supplementary Fig. 7j). Afterwards, doxycycline treatment was stopped for one cohort of mice (Fig. 2h), allowing recovery of *Cldn5* expression³³, which was confirmed at both mRNA and protein levels (Supplementary Fig. 7h). Recovery of normal *Cldn5* expression reversed anhedonia and promoted resilience in the social interaction test in stressed AAV-shRNA-Cldn5 mice (Fig. 2j). Conversely, stressed AAV-shRNA-Cldn5 mice in the second cohort remaining on doxycycline (Supplementary Fig. 7g) displayed anhedonia, social avoidance (Supplementary Fig. 7k) and lower *Cldn5* mRNA and Cldn5 protein levels (Supplementary Fig. 7i). These findings suggest that *Cldn5* expression plays a protective role in behavioral response to social stress, possibly by maintaining BBB impermeability to stress-induced passage of peripheral immune signals.

Chronic social stress alters blood vessel ultrastructure, promoting blood–brain barrier leakiness. Taking into account CSDS-induced loss of *Cldn5* and altered blood vessel morphology in SS mice, we next compared BBB integrity in CTRL, SS and RES mice following 10-d CSDS using a gadolinium contrast agent (Gd-DTPA, 0.7 kDa) and magnetic resonance imaging (MRI) scans (Fig. 3a and Supplementary Fig. 8a–c). Higher Gd-DTPA signal was detected in the NAc ($P=0.0237$) and hippocampus ($P=0.0085$) of SS mice compared to CTRL and RES mice (Fig. 3b), suggesting leakiness of the BBB in these brain areas. Accordingly, injection of AAV-shRNA-Cldn5 enhances passive diffusion of Gd-DTPA from the blood into the brain³³, reinforcing the role of *Cldn5* in maintaining BBB integrity under stressful conditions. Here we found that social avoidance was significantly correlated with Gd-DTPA level in the NAc ($P=0.0271$) (Fig. 3b,c and Supplementary Fig. 8d) and hippocampus ($P=0.0335$) (Fig. 3b and Supplementary Fig. 8d,e) but not PFC (Supplementary Fig. 8f). We confirmed stress-induced BBB leakiness in the NAc ($P=0.0022$) (Fig. 3d,e) and hippocampus of SS mice with cadaverine Alexa Fluor-555, a dye with a molecular weight of 0.95 kDa, which is similar to that of Gd-DTPA (Supplementary Fig. 8g–i). Again, accumulation of cadaverine Alexa Fluor-555 was significantly correlated with social avoidance (Supplementary Fig. 8j,k). Next we examined infiltration of Evans blue (EB) dye

following 10-d CSDS in stress-related brain regions. EB has a high affinity for serum albumin (~69 kDa) (Fig. 3e, left), which cannot readily cross the BBB in the absence of neurovascular damage. We measured a significant infiltration of EB in the NAc of SS mice ($P=0.0014$) when compared to CTRL and RES groups (Fig. 3e), and EB level correlated with social avoidance behavior ($P=0.0018$) (Supplementary Fig. 9a–d). The dye seemed to accumulate in the perivascular space of NAc blood vessels but not within the brain parenchyma (Fig. 3e, right). Notably, no significant accumulation of EB was observed in the hippocampus or PFC of defeated mice (Supplementary Fig. 9e–h), suggesting that the NAc BBB may be more vulnerable to neurovascular damage than that of other brain regions, leading to greater infiltration of larger proteins following stress. We confirmed BBB leakiness in the NAc of AAV-shRNA-Cldn5-injected adult mice by injecting Alexa Fluor-555-conjugated cadaverine (two-way ANOVA virus effect $P=0.0356$) and EB (two-way ANOVA virus effect $P<0.0001$), an effect exacerbated by stress (two-way ANOVA stress effect $P=0.0293$) (Fig. 3f–h). Finally, we compared the distribution of horseradish peroxidase (HRP, ~44 kDa) by transmission electron microscopy following 10-d CSDS. We found increased HRP uptake in the endothelium of SS mice ($P=0.0008$) (Fig. 3i). Together, these observations indicate that BBB integrity is impaired in SS but not RES mice, in line with a loss of *Cldn5* and abnormal blood vessel ultrastructure.

Previous studies report conflicting findings with regard to infiltration of peripheral immune cells into the brain following social stress^{14,34}. Considering the impact of 10-d CSDS on BBB permeability in the NAc of SS mice, we addressed this question by evaluating whether peripheral C-C chemokine receptor 2-expressing (*Ccr2*⁺) monocytes can infiltrate the brain parenchyma in stress-related brain regions. CSDS (10 d) induced drastic changes in cytokine and chemokine mRNA expression in the NAc of defeated animals (Fig. 1b,c), including a significant increase of *Ccr2* in SS mice ($P<0.0001$), which correlated with social avoidance ($P=0.0025$) (Supplementary Fig. 9i). We took advantage of *Ccr2*^{RFP}::*Cx3cr1*^{GFP} double heterozygous mice³⁵ in which adult resident microglia exhibit a *Ccr2*^{RFP}::*Cx3cr1*^{GFP+} pattern^{35,36} whereas peripheral monocytes, which are recruited in response to inflammation, are characterized by a *Ccr2*^{RFP+}::*Cx3cr1*^{GFP-} pattern^{35–37}. *Ccr2*^{RFP}::*Cx3cr1*^{GFP} mice were subjected to 10-d CSDS, followed by an SI test. Half of the brain was collected for flow cytometry analyses and the other half fixed for immunohistochemistry (IHC) (Fig. 4a). As expected, stressed mice displayed social avoidance when compared to unstressed controls ($P=0.0103$) (Fig. 4b and Supplementary Fig. 9j). Flow cytometry revealed more *Ccr2*^{RFP+}::*Cx3cr1*^{GFP-} peripheral monocytes in the brain of stressed bitransgenic mice compared to unstressed controls ($P=0.0479$) (Fig. 4c), with no change in *Ccr2*^{RFP}::*Cx3cr1*^{GFP+} resident microglia (Supplementary Fig. 9k,l). However, further analysis by IHC revealed that peripheral monocytes accumulated within ventricular space and NAc blood vessels, but did not infiltrate the brain parenchyma (Supplementary Fig. 9m).

Next we evaluated whether circulating IL-6 (~21 kDa), a pro-inflammatory cytokine associated with stress vulnerability and MDD^{7,11}, can infiltrate the NAc of defeated mice. We previously reported a 27-fold increase in circulating IL-6 level 20 min after defeat in SS mice¹¹. No difference in basal IL-6 was observed before stress, and IL-6 remained elevated in SS mice 48 h after the last defeat¹¹. Following 10-d CSDS (Supplementary Fig. 10a), we first confirmed higher IL-6 protein in the blood of SS mice 48 h after the last defeat (Fig. 4d). We also found higher IL-6 protein in NAc compared to that in unstressed CTRL mice ($P=0.0321$) (Fig. 4d), although this does not rule out the possibility that stress induces local production of IL-6. No difference was observed for hippocampus and PFC (Supplementary Fig. 10b), suggesting a region-specific accumulation of IL-6 in the NAc of SS mice following CSDS. To determine whether peripheral IL-6 is able to penetrate the brain

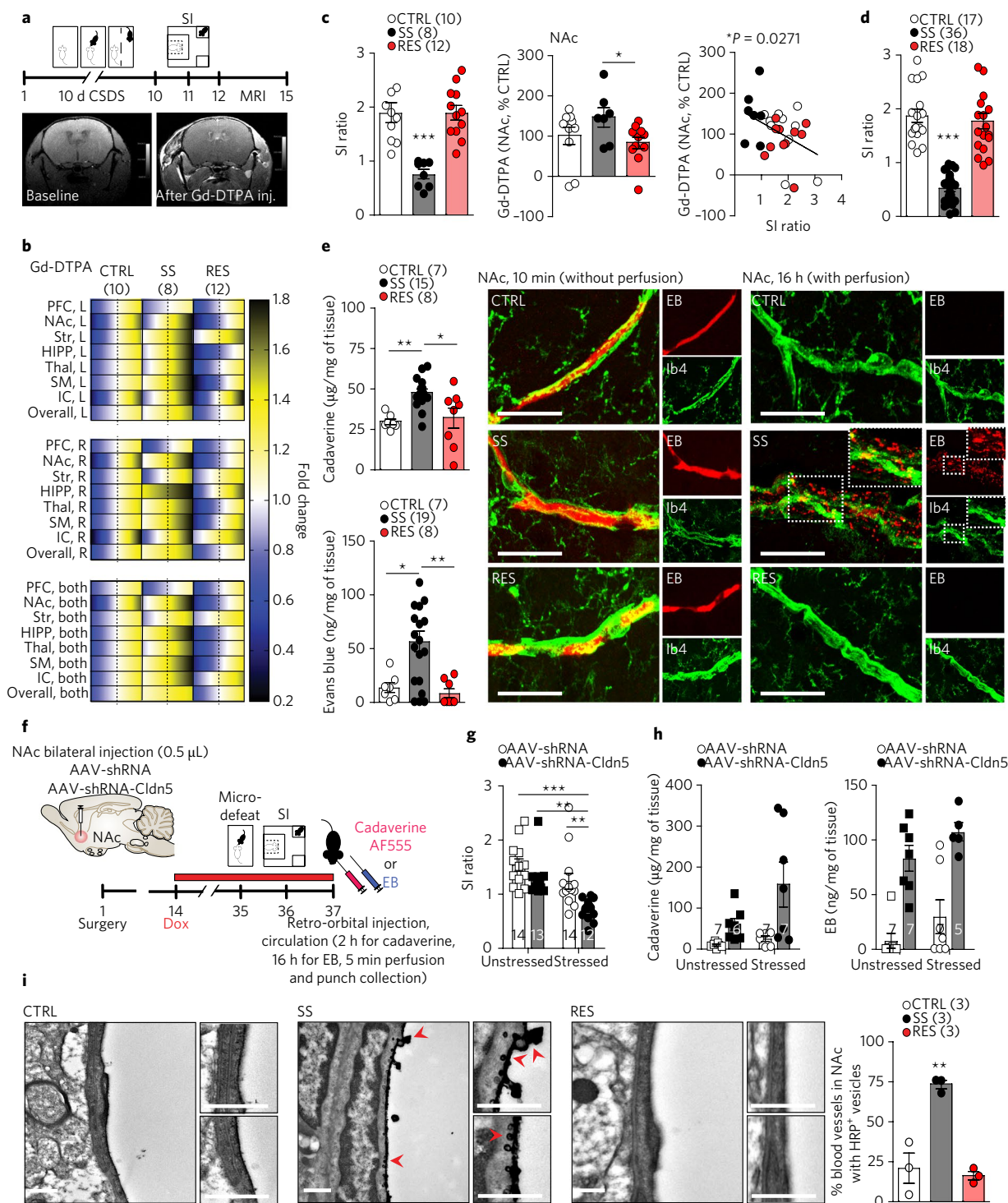


Fig. 3 | Social stress vulnerability is associated with increased BBB permeability. **a**, Experimental timeline of 10-d CSDS, SI screening and MRI scans. Pictures display baseline MRI scan compared to 25 min after injection (inj.) of Gd-DTPA. **b,c**, Higher Gd-DTPA signal was detected in different brain regions, including the NAc, in SS mice (**b**) and negatively correlated with SI ratio (**c**). The range of color in **b** indicates individual differences within a group; s.e.m. from the average represented by the dashed line. PFC, prefrontal cortex; NAc, nucleus accumbens; Str, striatum; HIPP, hippocampus; Thal, thalamus; SM, sensory motor cortex; IC, insular cortex; R, right; L, left. **d,e**, Assessment of BBB permeability with cadaverine Alexa Fluor-555 and Evans blue (EB) dyes revealed significant BBB leakiness in the NAc of SS mice. EB is present in all vessels within 10 min of injection and before perfusion (**e**, left) but can only be detected in the perivascular space of NAc blood vessels in SS mice after circulating 16 h followed by 5 min perfusion (**e**, right). Ib4, isolectin b4. Scale bars, 20 μ m. **f-h**, Downregulation of Cldn5 expression as described on the timeline (**f**) induced social avoidance (**g**) and increased BBB permeability to cadaverine Alexa Fluor-555 (AF555) and EB dyes (**h**) in AAV-shRNA-Cldn5 mice. **i**, Transmission electron microscopy, conducted 2 h after injection of HRP followed by 20 min perfusion, confirmed increased BBB permeability in the NAc of SS mice, with HRP detected within the endothelial cell lining (red arrows). Quantification was performed on 34–61 blood vessels per mouse in 3 mice per group. Scale bars, 500 nm. Data represent mean \pm s.e.m.; number of animals (*n*) is indicated on graphs. Correlations were evaluated with Pearson's correlation coefficient, two-way ANOVA followed by Bonferroni's multiple comparison test for BBB permeability in virus-injected mice, one-way ANOVA followed by Bonferroni's multiple comparison test for other graphs, **P* < 0.05; ***P* < 0.01; ****P* < 0.001.

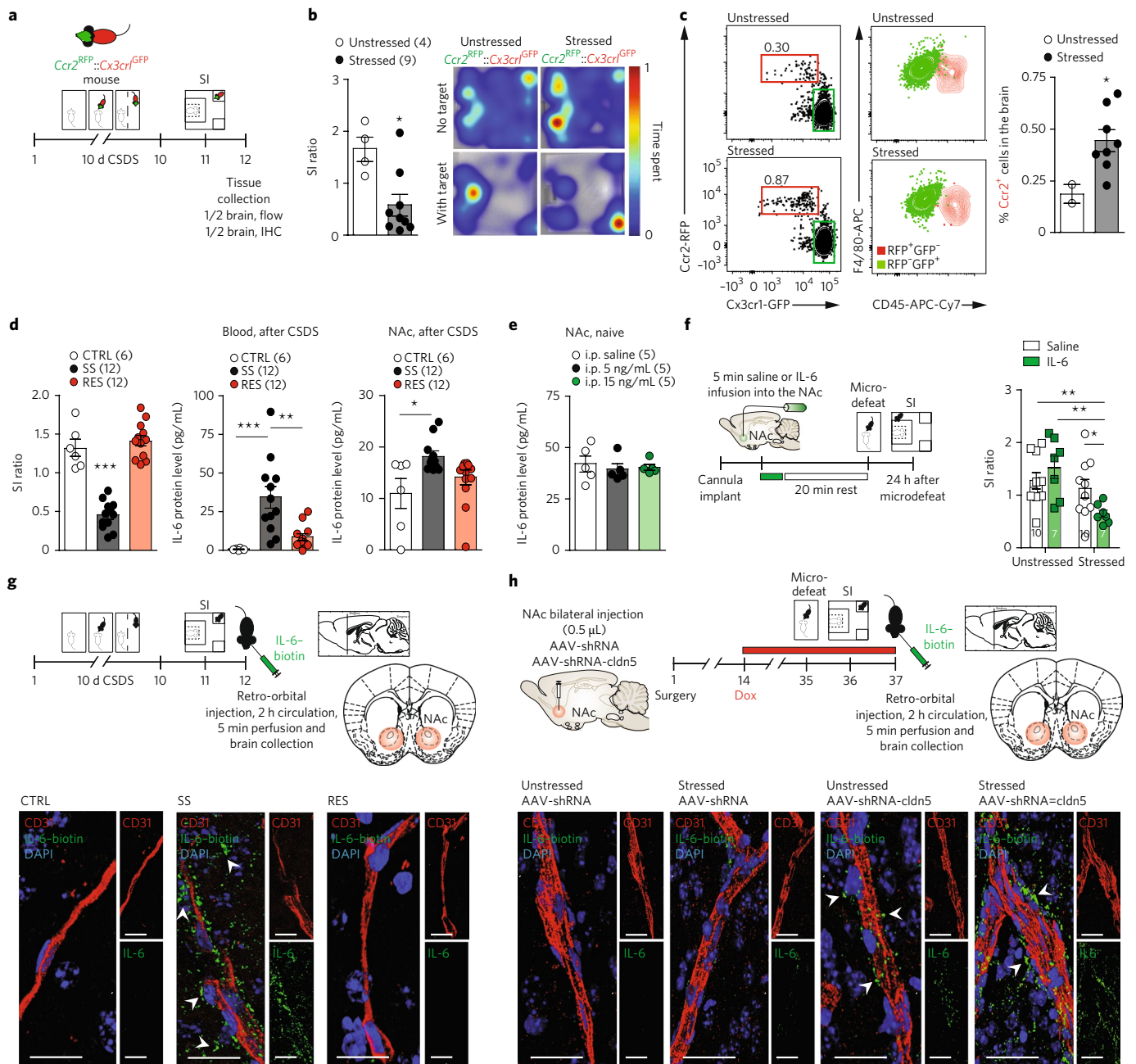


Fig. 4 | Chronic social stress induces peripheral monocyte accumulation and IL-6 passage into the NAc. **a**, Experimental timeline of 10-d CSDS, SI behavioral screening and tissue collection from *Ccr2*^{RFP::Cx3cr1}^{GFP} mice. **b**, Stressed *Ccr2*^{RFP::Cx3cr1}^{GFP} mice showed decreased SI scores (left) following 10-d CSDS. Representative heat maps are shown on the right. **c**, Flow cytometric analysis of forebrain *Ccr2*^{RFP} and *Cx3cr1^{GFP} cells revealed higher levels of *Ccr2*⁺ peripheral monocyte accumulation into the brains of stressed mice. Cells were gated on live *CD11b*⁺*F4/80*⁺ expression, where *F4/80* is a macrophage marker (left). Numbers adjacent to gates represent percentages of *Ccr2*⁺*Cx3cr1⁺ cells among *CD11b*⁺*F4/80*⁺ cells. Right panel shows *CD45* expression of *F4/80*⁺*Ccr2*⁺ monocytes and *F4/80*⁺*GFP*⁺ microglia. Bar graph shows percentage of *Ccr2*⁺*Cx3cr1⁺ cells among forebrain *CD11b*⁺*F4/80*⁺ cells. APC, allophycocyanin. **d**, IL-6 protein is increased in the blood and NAc of SS mice after 10-d CSDS. **e**, Dose increment of IL-6 i.p. injection did not change IL-6 protein levels in the NAc of stress-naive mice. **f**, Direct infusion of IL-6 into the NAc (5 min) induced social avoidance when subthreshold microdefeat was conducted 20 min after the end of the infusion. **g**, Top, experimental timeline of peripheral biotinylated IL-6 injection after 10-d CSDS. Bottom, IL-6-biotin/NeutrAvidin-Oregon 488-bound proteins were detectable in the NAc parenchyma of SS mice only after 2 h circulation and 5 min perfusion with PBS. Scale bars, 20 μ m. **h**, Top, experimental timeline. Bottom, biotinylated IL-6 was also detectable in the NAc of AAV-shRNA-*Cldn5*-injected mice. Scale bars, 20 μ m. Data represent mean \pm s.e.m.; number of animals (*n*) is indicated on graphs. *t*-test for *Cx3cr1^{GFP::Ccr2}^{RFP} mouse data, one-way ANOVA followed by Bonferroni's multiple comparison test for IL-6 protein levels and two-way ANOVA followed by Bonferroni's multiple comparison test for SI ratio after IL-6 or saline infusion, **P* < 0.05; ***P* < 0.01; ****P* < 0.001.****

parenchyma of SS mice, we tagged mouse recombinant IL-6 with biotin (~0.45 kDa) and injected it retro-orbitally into the blood of CTRL, SS or RES mice (Fig. 4g and Supplementary Fig. 10d–g). Two

hours later, animals were perfused and brains were collected, and the expression of biotinylated IL-6 in the brain was assessed using a NeutrAvidin Oregon-488-conjugated secondary antibody. Notably,

biotinylated IL-6 was only detectable in the NAc of SS mice, and labeling with the perivascular marker CD31 revealed passage outside of blood vessels into the parenchyma (Fig. 4g). Biotinylated IL-6 was undetectable in the hippocampus or PFC of SS mice (Supplementary Fig. 10f,g). Our studies also revealed that the NAc is largely impermeable to circulating IL-6 under normal conditions, as we were unable to detect biotinylated IL-6 in the NAc of unstressed CTRL mice (Fig. 4g) and i.p. injections of recombinant IL-6 did not increase levels of IL-6 in NAc of naive mice (Fig. 4e) despite there being a large increase in the blood of these mice (Supplementary Fig. 10c). Downregulation of *Cldn5* expression with an AAV-shRNA allowed the passage of biotinylated IL-6 into the NAc parenchyma (Fig. 4h). To confirm the importance of NAc IL-6 in the establishment of depression-like behaviors, we implanted cannulas in the NAc of stress-naive mice and infused either saline or IL-6 before subthreshold microdefeat (Fig. 4f). Stressed mice that received intra-NAc IL-6 displayed social avoidance compared to stressed mice receiving intra-NAc saline or unstressed mice receiving either intra-NAc IL-6 or saline ($P=0.0405$) (Fig. 4f and Supplementary Fig. 10h–j). These observations indicate that social stress causes direct passage of the pro-inflammatory cytokine IL-6, which then acts directly within the NAc to induce depression-like behaviors.

Discussion

Overall, our findings suggest that chronic social stress alters BBB integrity through downregulation of the tight junction protein *Cldn5* in the NAc, which, combined with stress-induced recruitment of peripheral immune signals, results in increased BBB permeability, passage of blood circulating proteins such as IL-6, and the development of depression-like behaviors (Supplementary Fig. 11). Our findings complement decades of correlative clinical evidence suggesting that the immune system and elevations in circulating pro-inflammatory cytokines, particularly IL-6, are involved in the establishment of MDD^{1,7,11,38,39}. We previously reported higher serum IL-6 in patients with untreated MDD and treatment-resistant MDD when compared to healthy controls^{11,40}. Though a potential link between BBB leakiness and depression was first proposed over 50 years ago⁴¹, the development of new tools, such as valid rodent models of depression and high-resolution imaging, have made it feasible to address this question. Our work highlights an important function of the BBB-related tight junction protein *Cldn5* as a regulator of stress-induced depression-like behaviors. While size-selective loosening of the BBB to small molecules (<800 Da) was previously described in *Cldn5*-deficient mice²³, we show here that chronic social stress can also loosen the BBB by downregulating *Cldn5*, allowing larger molecules to infiltrate the NAc parenchyma in SS mice.

Though we found increased passage of proteins of up to ~69 kDa, we did not detect infiltration of peripheral *Ccr2*⁺ monocytes as in a previous report¹⁴. This may be related to differences in social stress models or to our use of a bitransgenic mouse that allows simultaneous tracking of monocytes and microglia without generating chimeric mice through bone marrow transplantation. We nevertheless confirm a recent report showing that monocytes are recruited to vessels and ventricular space within the brain³⁴. From these vascular sites, monocytes can release pro-inflammatory cytokines, such as IL-6, that can then penetrate the brain parenchyma to act locally on neurons and glia. To our knowledge, this is the first study to provide direct evidence that chronic stress is sufficient to allow infiltration of circulating cytokines in the absence of local mechanical trauma or a brain tumor^{42,43}. Greater understanding of the mechanisms by which chronic stress activates the immune system and undermines BBB integrity may promote the design of more effective antidepressant strategies, either by augmenting current treatment protocols or by informing the discovery of new therapeutics that enhance neurovascular health in stress-related brain regions. A major impediment to this goal is the lack of therapeutic agents that can enhance

Cldn5 expression to repair endothelial damage as, so far, no such compound exists.

Methods

Methods, including statements of data availability and any associated accession codes and references, are available at <https://doi.org/10.1038/s41593-017-0010-3>.

Received: 28 June 2017; Accepted: 27 September 2017;

Published online: 13 November 2017

References

- Ménard, C., Pfau, M. L., Hodes, G. E. & Russo, S. J. Immune and neuroendocrine mechanisms of stress vulnerability and resilience. *Neuropsychopharmacology* **42**, 62–80 (2017).
- Kessler, R. C., Chiu, W. T., Demler, O., Merikangas, K. R. & Walters, E. E. Prevalence, severity, and comorbidity of 12-month DSM-IV disorders in the National Comorbidity Survey replication. *Arch. Gen. Psychiatry* **62**, 617–627 (2005).
- Seligman, F. & Nemeroff, C. B. The interface of depression and cardiovascular disease: therapeutic implications. *Ann. NY Acad. Sci.* **1345**, 25–35 (2015).
- Carney, R. M. & Freedland, K. E. Depression and coronary heart disease. *Nat. Rev. Cardiol.* **14**, 145–155 (2017).
- Wood, S. K. Individual differences in the neurobiology of social stress: implications for depression-cardiovascular disease comorbidity. *Curr. Neuropharmacol.* **12**, 205–211 (2014).
- Huffman, J. C., Celano, C. M., Beach, S. R., Motiwala, S. R. & Januzzi, J. L. Depression and cardiac disease: epidemiology, mechanisms, and diagnosis. *Cardiovasc. Psychiatry Neurol.* **2013**, 695925 (2013).
- Hodes, G. E., Kana, V., Menard, C., Merad, M. & Russo, S. J. Neuroimmune mechanisms of depression. *Nat. Neurosci.* **18**, 1386–1393 (2015).
- Barnes, J., Mondelli, V. & Pariante, C. M. Genetic contributions of inflammation to depression. *Neuropsychopharmacology* **42**, 81–98 (2017).
- Dantzer, R. Cytokine, sickness behavior, and depression. *Immunol. Allergy Clin. North Am.* **29**, 247–264 (2009).
- Miller, A. H. & Raison, C. L. The role of inflammation in depression: from evolutionary imperative to modern treatment target. *Nat. Rev. Immunol.* **16**, 22–34 (2016).
- Hodes, G. E. et al. Individual differences in the peripheral immune system promote resilience versus susceptibility to social stress. *Proc. Natl. Acad. Sci. USA* **111**, 16136–16141 (2014).
- Powell, N. D. et al. Social stress up-regulates inflammatory gene expression in the leukocyte transcriptome via β -adrenergic induction of myelopoiesis. *Proc. Natl. Acad. Sci. USA* **110**, 16574–16579 (2013).
- Heidt, T. et al. Chronic variable stress activates hematopoietic stem cells. *Nat. Med.* **20**, 754–758 (2014).
- Wohleb, E. S., Powell, N. D., Godbout, J. P. & Sheridan, J. F. Stress-induced recruitment of bone marrow-derived monocytes to the brain promotes anxiety-like behavior. *J. Neurosci.* **33**, 13820–13833 (2013).
- Weber, M. D., Godbout, J. P. & Sheridan, J. F. Repeated social defeat, neuroinflammation, and behavior: monocytes carry the signal. *Neuropsychopharmacology* **42**, 46–61 (2017).
- Esposito, P. et al. Acute stress increases permeability of the blood-brain-barrier through activation of brain mast cells. *Brain Res.* **888**, 117–127 (2001).
- Sántha, P. et al. Restraint stress-induced morphological changes at the blood-brain barrier in adult rats. *Front. Mol. Neurosci.* **8**, 88 (2016).
- Friedman, A. et al. Pyridostigmine brain penetration under stress enhances neuronal excitability and induces early immediate transcriptional response. *Nat. Med.* **2**, 1382–1385 (1996).
- Sharma, H. S. & Dey, P. K. Impairment of blood-brain barrier (BBB) in rat by immobilization stress: role of serotonin (5-HT). *Indian J. Physiol. Pharmacol.* **25**, 111–122 (1981).
- Niklasson, F. & Agren, H. Brain energy metabolism and blood-brain barrier permeability in depressive patients: analyses of creatine, creatinine, urate, and albumin in CSF and blood. *Biol. Psychiatry* **19**, 1183–1206 (1984).
- Roszkowski, M. & Bohacek, J. Stress does not increase blood-brain barrier permeability in mice. *J. Cereb. Blood Flow Metab.* **36**, 1304–1315 (2016).
- Günzel, D. & Yu, A. S. Claudins and the modulation of tight junction permeability. *Physiol. Rev.* **93**, 525–569 (2013).
- Nitta, T. et al. Size-selective loosening of the blood-brain barrier in claudin-5-deficient mice. *J. Cell Biol.* **161**, 653–660 (2003).
- Meltzer, H., Vostanis, P., Ford, T., Bebbington, P. & Dennis, M. S. Victims of bullying in childhood and suicide attempts in adulthood. *Eur. Psychiatry* **26**, 498–503 (2011).
- Berton, O. & Nestler, E. J. New approaches to antidepressant drug discovery: beyond monoamines. *Nat. Rev. Neurosci.* **7**, 137–151 (2006).
- Ménard, C., Hodes, G. E. & Russo, S. J. Pathogenesis of depression: Insights from human and rodent studies. *Neuroscience* **321**, 138–162 (2016).

27. Golden, S. A., Covington, H. E. III, Berton, O. & Russo, S. J. A standardized protocol for repeated social defeat stress in mice. *Nat. Protoc.* **6**, 1183–1191 (2011).
28. Russo, S. J. & Nestler, E. J. The brain reward circuitry in mood disorders. *Nat. Rev. Neurosci.* **14**, 609–625 (2013).
29. Zhang, Y. et al. An RNA-sequencing transcriptome and splicing database of glia, neurons, and vascular cells of the cerebral cortex. *J. Neurosci.* **34**, 11929–11947 (2014).
30. Zhang, Y. et al. Purification and characterization of progenitor and mature human astrocytes reveals transcriptional and functional differences with mouse. *Neuron* **89**, 37–53 (2016).
31. Hodes, G. E. et al. Sex differences in nucleus accumbens transcriptome profiles associated with susceptibility versus resilience to subchronic variable stress. *J. Neurosci.* **35**, 16362–16376 (2015).
32. Golden, S. A. et al. Epigenetic regulation of RAC1 induces synaptic remodeling in stress disorders and depression. *Nat. Med.* **19**, 337–344 (2013).
33. Campbell, M. et al. Systemic low-molecular weight drug delivery to pre-selected neuronal regions. *EMBO Mol. Med.* **3**, 235–245 (2011).
34. McKim, D.B. et al. Microglial recruitment of IL-1 β -producing monocytes to brain endothelium causes stress-induced anxiety. *Mol. Psychiatry* <https://doi.org/10.1038/mp.2017.64> (2017).
35. Saederup, N. et al. Selective chemokine receptor usage by central nervous system myeloid cells in CCR2-red fluorescent protein knock-in mice. *PLoS One* **5**, e13693 (2010).
36. Mizutani, M. et al. The fractalkine receptor but not CCR2 is present on microglia from embryonic development throughout adulthood. *J. Immunol.* **188**, 29–36 (2012).
37. Ginhoux, F. & Jung, S. Monocytes and macrophages: developmental pathways and tissue homeostasis. *Nat. Rev. Immunol.* **14**, 392–404 (2014).
38. Maes, M. et al. Increased serum IL-6 and IL-1 receptor antagonist concentrations in major depression and treatment resistant depression. *Cytokine* **9**, 853–858 (1997).
39. Dowlati, Y. et al. A meta-analysis of cytokines in major depression. *Biol. Psychiatry* **67**, 446–457 (2010).
40. Kiraly, D. D. et al. Altered peripheral immune profiles in treatment-resistant depression: response to ketamine and prediction of treatment outcome. *Transl. Psychiatry* **7**, e1065 (2017).
41. Coppen, A. J. Abnormality of the blood-cerebrospinal fluid barrier of patients suffering from a depressive illness. *J. Neurol. Neurosurg. Psychiatry* **23**, 156–161 (1960).
42. Hambardzumyan, D., Gutmann, D. H. & Kettenmann, H. The role of microglia and macrophages in glioma maintenance and progression. *Nat. Neurosci.* **19**, 20–27 (2016).
43. Shichita, T. et al. Pivotal role of cerebral interleukin-17-producing $\gamma\delta$ T cells in the delayed phase of ischemic brain injury. *Nat. Med.* **15**, 946–950 (2009).

Acknowledgements

The authors thank A. Keller for advice on BBB-related studies and the Center for Comparative Medicine and Surgery housing facilities staff for their work and support. This research was supported by Mental Health grants RO1 MH090264 (S.J.R.), P50 MH096890 (S.J.R.), P50 AT008661-01 (S.J.R.), RO1 MH114882 (S.J.R.), RO1 MH104559 (S.J.R. and M.M.), NIH/NHLBI P01 HL131478 (Z.A.F.), T32 MH087004 (M.L.P., M.H. and M.F.), T32 MH096678 (M.L.P.), F30 MH100835 (M.H.) and F31 MH105217 (M.L.P.), a Janssen/IMHRO Rising Star Translational Research Award (S.J.R.), a Swiss National Science Foundation Advanced Postdoc Mobility Fellowship (V.K.) and a Brain and Behavior Research Foundation NARSAD Young Investigator Award (G.E.H.). C.M. is supported by a Brain and Behavior Research Foundation NARSAD Young Investigator Grant sponsored by the P&S Fund.

Author contributions

C.M. and S.J.R. designed the study and wrote the manuscript. C.M., M.L.P., G.E.H., A.T., M.E.F., H.A., K.B.L., Z.S.L., S.A.G. and M.H. performed stereotaxic surgeries, tissue collection and behavioral manipulations and analyzed data. V.K. performed and analyzed flow experiments and *Ccr2^{RFPP}::Cx3cr1^{GFP}* mouse immunostaining. V.K. and M.M. provided *Ccr2^{RFPP}::Cx3cr1^{GFP}* mice and provided advice on BBB- and immune-related studies. V.X.W., Z.A.F. and C.Y.T. designed, performed and analyzed magnetic resonance imaging scans. S.B. advised on analysis approaches and analyzed data. W.G.J. prepared and imaged transmission electron microscopy samples. B.L., E.M.P., C.T. and G.T. provided post-mortem human tissue samples. M.C. provided viral vectors and advised on viral studies. All the authors read and commented on the manuscript.

Competing interests

The authors declare no competing financial interests.

Additional information

Supplementary information is available for this paper at <https://doi.org/10.1038/s41593-017-0010-3>.

Reprints and permissions information is available at www.nature.com/reprints.

Correspondence and requests for materials should be addressed to S.J.R.

Publisher's note: Springer Nature remains neutral with regard to jurisdictional claims in published maps and institutional affiliations.

Methods

Mice. Male C57BL/6J mice (~25 g) were purchased at 7 weeks of age from the Jackson Laboratory and allowed 1 week of acclimation to the Icahn School of Medicine at Mount Sinai (ISMMS) housing facilities before the start of experiments. *Ccr2^{RFP}::Cx3cr1^{GFP}* mice were bred at the ISMMS facilities and used at 8–10 weeks of age. Sexually experienced retired male CD-1 breeders (~40 g) at least 4 months of age were purchased from Charles River Laboratories and used as aggressors (AGG). All mice were singly housed following CSDS and maintained on a 12-h/12-h light/dark cycle throughout. Mice were provided with ad libitum access to water and food except during the novelty-suppressed feeding test. Behavioral assessments and tissue collection were performed into the dark phase. All mouse procedures were performed in accordance with the National Institutes of Health Guide for Care and Use of Laboratory Animals and the ISMMS Animal Care and Use Committee.

Chronic social defeat stress (CSDS). CSDS was performed as previously described^{11,27,32}. CD-1 mice were screened for aggressive behavior during inter-male social interactions for 3 consecutive days on the basis of previously described criteria^{27,44} and housed in the social defeat cage (26.7 cm width × 48.3 cm depth × 15.2 cm height, Allentown Inc) 24 h before the start of defeats (day 0) on one side of a clear perforated Plexiglas divider (0.6 cm × 45.7 cm × 15.2 cm, Nationwide Plastics). Experimental C57BL/6J or *Ccr2^{RFP}::Cx3cr1^{GFP}* mice were subjected to physical interactions with an unfamiliar CD-1 AGG for 10 min once per day over 10 consecutive days. After antagonistic interactions, experimental mice were removed and housed on the opposite side of the social defeat cage divider, allowing sensory contact, over the subsequent 24-h period. Unstressed control mice were housed two per cage in either side of a perforated divider and rotated daily in a similar manner without being exposed to the CD-1 AGG mice. Experimental mice were singly housed after the last bout of physical interaction and the social interaction (SI) test was conducted 24 h later.

Microdefeat stress. A subthreshold variation of the CSDS protocol was used to evaluate increased susceptibility to stress^{1,32}. Experimental C57BL/6J mice were exposed to physical interactions with a new CD-1 AGG for three consecutive bouts of 5 min, with a 15-min rest period between each bout. The SI test was conducted 24 h later.

Social interaction/avoidance test. SI testing was performed as previously described under red-light conditions^{11,27,32}. First, mice were placed in a Plexiglas open-field arena (42 cm × 42 cm × 42 cm, Nationwide Plastics) with a small wire animal cage placed at one end. Movements were monitored and recorded automatically for 2.5 min with a tracking system (Ethovision 11.0 Noldus Information Technology) to determine baseline exploratory behavior and locomotion in the absence of a social target (AGG). At the end of 2.5 min, the mouse was removed and the arena cleaned. Next, exploratory behavior in the presence of a novel social target inside the small wire animal cage was measured for 2.5 min and time spent in the interaction and corner zones and overall locomotion were compared. SI ratio was calculated by dividing the time spent in the interaction zone when the AGG was present divided by the time spent in the interaction zone when the AGG was absent. All mice with a SI ratio below 1.0 were classified as stress-susceptible (SS) and all mice with a SI ratio above 1.0 were classified as resilient (RES).

Splash test. The splash test was used to compare grooming behavior in stressed versus unstressed virus-injected mice under red-light conditions as described previously³¹. A 10% sucrose solution was sprayed on the lower back of the mice and time spent grooming was videotaped and then calculated with a stop watch.

Sucrose preference test. Anhedonic responses of stressed versus unstressed virus-injected mice were evaluated with a standard sucrose preference assay. Water bottles from home cages were removed and replaced with two 50-mL conical tubes with sipper tops filled with water for a 24-h habituation period. Next, water from one of the 50-mL conical tube was replaced with a 1% sucrose solution. All tubes were weighed and mice were allowed to drink ad libitum for a 24-h period. Tubes were then reweighed and switched for another 24-h period of ad libitum drinking to prevent place preference. At the end of the 48-h testing, sucrose preference was calculated by dividing the total amount of sucrose consumed by the total amount of fluid consumed over the 2 d of sucrose availability.

Forced swim test. Mice were placed into a 4-L glass beaker filled with 3 L of water at 25°C under bright light conditions and videotaped for 6 min. Time spent immobile was measured with a stop watch. Immobility was defined as no movement at all or only minor movements necessary to keep the nose above the water versus mobility, which was defined by swimming and struggling behaviors.

Novelty-suppressed feeding. This test assesses stress-induced anxiety by measuring aversion to feed in a novel environment despite food deprivation. Virus-injected stressed or unstressed mice were food-deprived overnight (with ad libitum access to water) and then placed in the corner of an unfamiliar white Plexiglas

arena (42 cm × 42 cm × 42 cm, Nationwide Plastics) with the floor covered in corn cob bedding under red-light conditions. A food pellet was prepositioned in the middle of the arena. Latency to eat was measured with a stopwatch and defined by the first bite into the food pellet. Maximum time allowed was set at 10 min.

Elevated plus maze. Mice were placed in a black Plexiglas cross-shaped elevated plus maze (arms of 12 cm width × 50 cm length) under red-light conditions for 5 min. The maze consists of a center area, two opens arms with no wall and two closed arms with 40-cm high walls set on a pedestal 1 m above floor level. Locomotion was monitored and tracked using an automated system (Ethovision 11.0 Noldus Information Technology). Cumulative time spent in open arms, center and closed arms was compared between groups.

Open field. Mice were placed in a white Plexiglas open-field arena (42 cm × 42 cm × 42 cm, Nationwide Plastics) and locomotion was monitored and tracked using an automated system (Ethovision 11.0 Noldus Information Technology) for 10 min. An area of 10 cm × 10 cm was defined as the center and an adjacent 20 cm × 20 cm area was defined as the middle or non-periphery. The area along the walls was defined as the periphery. Cumulative time spent in each area was compared between groups.

Transcriptional profiling. Nucleus accumbens (NAc), hippocampus or prefrontal cortex (PFC) samples were collected and processed as described previously³². Bilateral 14-gauge punches were collected from 1-mm coronal slices on wet ice after rapid decapitation and immediately placed on dry ice and stored at -80°C until use. RNA was isolated using TRIzol (Invitrogen) homogenization and chloroform layer separation. The clear RNA layer was processed with RNeasy MicroKit (Qiagen), analyzed with NanoDrop (Thermo Fisher Scientific) and 500 ng of RNA reverse transcribed to cDNA with qScript (Quanta Biosciences). The resulting cDNA was then diluted to 500 µl and 3 µl was used for each quantitative PCR reaction with 5 µl of Perfecta SYBR Green (Quanta Biosciences), forward and reverse primers (0.5 µl each or 1 µl for PrimeTime qPCR primers) and 1 µl of water. Samples were heated to 95°C for 2 min followed by 40 cycles of 95°C for 15 s, 60°C for 33 s and 72°C for 33 s. Analysis was done using the ΔΔC_t method and samples were normalized to the *Gapdh* (mouse) or *GAPDH* (human) housekeeping gene. Primer pairs (Integrated DNA Technologies) are listed in Supplementary Tables 1, 3 and 4.

Immunohistochemistry (IHC) and quantification of tight junction proteins. Mice were anesthetized with a mixture of ketamine (100 mg/kg of body weight) and xylazine (10 mg/kg of body weight), perfused for 7 min with 0.1 M PBS and the brains quickly extracted and frozen in OCT Compound (Fisher Scientific) using isopentane on dry ice. Immunostaining was performed according to Mishra et al.⁴⁵ with minor modifications. Briefly, blocks were stored at -20°C for 24 h before slicing on a cryostat at 12 µm thickness. Slices were postfixed for 10 min in ice-cold methanol before a quick wash in 0.1 M PBS. Sections were then incubated for 2 h in 5% normal donkey serum (NDS) in 0.1 M PBS before overnight incubation with primary antibodies^{46–48} (rabbit anti-Cldn5, 1:100, Life Technologies, #34-1600; rabbit anti-occludin, 1:250, Life Technologies, #40-4700; rabbit anti-ZO-1, 1:50; Life Technologies, #61-7300) in 1% NDS in 0.1 M PBS. Double immunostaining with CD31 (anti-rat-CD31, 1:150, BD Biosciences, #5550274) was performed to allow localization of blood vessels for quantification of tight junctions protein levels. After three washes in PBS for 10 min, sections were incubated with anti-rabbit-Cy2 and anti-rat-Cy5 secondary antibodies for 2 h (1:400, Jackson ImmunoResearch, #711-225-152, #712-175-153, respectively), washed again three times with PBS and stained with 4,6-diamidino-2-phenylindole (DAPI) to visualize nuclei. Slices were mounted and coverslipped with ProLong Diamond Antifade Mountant (Invitrogen). One-micrometer-thick z-stack images of the NAc, hippocampus or PFC were acquired on a LSM-780 confocal microscope (Carl Zeiss). Images were taken using a 40× lens with a resolution of 1,056 × 288 and a zoom of 2.0. Pixel size was 0.1 µm in the x-y-z planes, pixel dwell time was 1.58 µs and the line average was set at 2. Flattened z-stack average intensity was compared using Image J (NIH) with the region of interest (ROI) defined using CD31 staining.

IHC for Evans blue (EB). Staining with the perivascular marker isolectin B4 (Ib4) and intravascular Evans blue (EB) were performed as previously described⁴⁹, followed by Cldn5 indirect immunostaining³³. Mice were anesthetized with a mixture of ketamine (100 mg/kg of body weight) and xylazine (10 mg/kg of body weight) and administered 6 µl/g of body weight 2% (wt/vol) EB (Sigma) dissolved in saline through retro-orbital injection. After 10 min, the mouse was decapitated and the brain was collected and fixed in 15 mL freshly prepared, cold 4% paraformaldehyde (PFA) plus 0.05% glutaraldehyde. Brains were then cryoprotected in 30% sucrose, frozen and sliced on a cryostat at 40 µm thickness. Slices were washed in 0.1 M phosphate-buffered saline (PBS) and antigen retrieval was performed as described in ref.⁴⁹ before incubation for 72 h at 4°C with biotinylated Ib4 (1:50, Sigma) in CaCl₂-containing buffer and blocking solution (0.05% Triton X-100 and 2% NDS). After three washes in PBS for 10 min, sections were incubated with streptavidin-Cy3 (1:500, Sigma, #S6402) secondary antibody in CaCl₂-containing buffer and blocking solution (0.05% Triton X-100

and 2% NDS) for 24 h. Sections were washed again three times with PBS and stained with DAPI to visualize nuclei. Slices were mounted and coverslipped with ProLong Diamond Antifade Mountant (Invitrogen). Ten-micrometer-thick z-stack images of the NAc, hippocampus or PFC were acquired on a LSM-780 confocal microscope (Carl Zeiss). Images were taken using a 40× lens with a resolution of 1,056 × 288 and a zoom of 2.0. Pixel size was 0.1 μm in the x-y-z planes, pixel dwell time was 1.58 μs and the line average was set at 2.

Capillary extraction and western blot. For whole homogenate samples, a half brain of a naive mouse was collected and homogenized in RIPA lysis buffer (Sigma) containing phosphatase and protease inhibitor cocktails (Sigma). For capillary extraction, a half brain of a naive mouse was homogenized in 1 mL of cold DMEM using a Dounce homogenizer and then centrifuged at 4,000g for 5 min at 4°C. The supernatant was removed and the pellet was resuspended in 18% dextran solution diluted in 0.1 M PBS as previously described⁴⁹. After centrifugation (6,000g for 10 min at 4°C), the supernatant and myelin debris floating at the surface were removed. The pellet was resuspended in DMEM supplemented with 1 mg/mL collagenase/dispase (collagenase: 0.1 U/mL; dispase: 0.8 U/mL), 40 μg/mL DNase I and 0.147 μg/mL tosyllysine chloromethyl ketone (Sigma) and incubated at 37°C for 75 min with agitation to free endothelial cells from pericytes, perivascular macrophages and remains of the basement membrane. After centrifugation (4,000g for 10 min at room temperature), the supernatant was discarded and the pellet was resuspended in RIPA lysis buffer. All samples were centrifuged at 21,000g for 30 min at 4°C before protein quantification with Microplate BCA Protein Assay Kit (Bio-Rad Laboratories). Equal amounts of protein samples were separated by SDS-PAGE (Bio-Rad 4–20% polyacrylamide gels) and transferred to PVDF membranes (Bio-Rad). The membranes were blocked with 5% bovine serum albumin (BSA) in 0.1 M PBS and incubated overnight with primary antibodies against Cldn5 (1:1,000, rabbit, Life Technologies, #34-1600), glial fibrillary acidic protein (GFAP; 1:1,000, guinea pig, Synaptic Systems, #173 004) or NeuN (1:1,000, mouse, Millipore, MAB377). After four 10-min washes with Tris-buffered saline supplemented with Tween 20 (TBST), membranes were incubated for 2 h with secondary antibodies (1:5,000, Vector Laboratories goat anti-rabbit #PI-1000; Life Technologies, goat anti-mouse #G-21040, goat anti-guinea pig, #A18769). Membranes were washed four more times with TBST and then antibody binding was detected using SuperSignal West Dura Supplementary Duration Substrate (Thermo Fisher Scientific) and a Bio-Rad Molecular Imager ChemiDoc XRS detection system with Image Lab software. Quantification was performed with Image J (NIH).

For virus validation, bilateral NAc punches were combined and homogenized in a RIPA lysis buffer (Sigma) containing phosphatase and protease inhibitor cocktails (Sigma). All samples were centrifuged at 21,000g for 30 min at 4°C before protein quantification with DCA Protein Assay Kit (Bio-Rad Laboratories). Equal amounts of protein samples were separated by SDS-PAGE (Bio-Rad 4–20% polyacrylamide gels) and western blots for Cldn5 and actin were performed as described above. Full-length western blots are available in Supplementary Figs. 2 and 12.

Imipramine treatment. Following the SI test, unstressed CTRL and SS mice were randomly divided into either vehicle or imipramine treatment groups. Each mouse received daily i.p. injections³² of imipramine (20 mg/kg of body weight) or vehicle for 35 d. All mice were screened again for social avoidance before tissue collection. Mice were then killed 24 h after the last injection and bilateral 14-gauge NAc tissue punches were collected from 1-mm-thick coronal slices for quantitative PCR as described previously.

Transmission electron microscopy (TEM). Mice were screened for behavioral phenotype with the SI test (CTRL, SS or RES) after 10-d CSDS and TEM was performed. Mice were administered horseradish peroxidase type II (HRP, Sigma, 100 mg/mL in PBS, 10 mg/20 g of body weight) through retro-orbital injection 24 h after SI test screening. HRP was allowed to circulate for 2 h, and animals were overdosed using 100 mg/kg sodium pentobarbital and transcardially perfused using ice-cold 0.1 M PBS (pH 7.3) at a flow rate of 7.5–8 mL/min for 60 s (until liver was completely cleared) followed with 2.5% glutaraldehyde in 0.1 M PBS (pH 7.3) for 12 min at a flow rate of 7.5–8 mL/min. Brains were removed, postfixed in the same fixative as above and stored at 4°C until ready for IHC. For morphology studies, samples were washed in 0.1 M sodium cacodylate buffer, postfixed in 1% osmium tetroxide/0.1 M cacodylate buffer, washed and dehydrated through a graduated ethanol to propylene oxide series, and resin infiltrated with Epon (Electron Microscopy Sciences). Material was vacuum oven polymerized at 60°C for 48 h. Semi-thick (1-μm) toluidine blue sections were used to identify the final ROI. Ultrathin sections (80 nm) were cut with a diamond knife (Diatome) with sections collected on 300-mesh copper grids (Electron Microscopy Sciences). Sections were counterstained with uranyl acetate and lead citrate. For BBB permeability assessment, an HRP-diaminobenzidine reaction (Vector Laboratories) was performed for 5 min on 200-μm coronal slices sectioned using a Vibratome (Leica, VT1000S). Reacted tissue was embedded as previously described⁵¹. Briefly, slices were cryoprotected with graded PB/glycerol (10, 20 and 30%) washes at 4°C and manually microdissected to obtain blocks containing the ROI. Blocks were

rapidly freeze-plunged into liquid propane cooled by liquid nitrogen (−90°C) in a Universal Cryofixation System KF80 (Reichert-Jung) and subsequently immersed in 1.5% uranyl acetate dissolved in anhydrous methanol at −90°C for 24 h in a cryosubstitution unit (Leica). Block temperatures were raised from −90°C to −45°C in steps of 4°C/h and the blocks were washed with anhydrous methanol and infiltrated with Lowicryl resin (Electron Microscopy Sciences) at −45°C. The resin was polymerized by exposure to ultraviolet light (360 nm) for 48 h at −45°C followed by 24 h at 0°C. Using an EMUC7 ultramicrotome (Leica Microsystems Inc.), block faces were trimmed using a histo-knife (Diatome), and semi-thick (1-μm) toluidine blue sections were used to identify the final ROI. Ultrathin sections (90 nm) were cut with a diamond knife (Diatome) and sections collected on formvar/carbon-coated nickel slot grids (Electron Microscopy Sciences). Images were taken using a Hitachi 7000 electron microscope (Hitachi High-Technologies Corporation America, Inc.) and imported to Photoshop for final brightness and contrast adjustment and sizing. Quantification was performed using ImageJ software (NIH). All blood vessels on the sample were imaged at a low and high magnification, with a total minimum of 100 images per animal (grid) sampled.

Human post-mortem tissue collection. Whole-tissue NAc, hippocampus or PFC (BA25) resections were collected and provided by the Quebec Suicide Brain Bank at the Douglas Hospital Research Center (McGill University) under approval of the institution's Ethics Committee for the Montreal cohort³². For the Texas cohort, whole-tissue NAc resections were collected and provided by the Dallas Brain Collection (tissue was collected by the Dallas Medical Examiner's Office and the University of Texas Southwestern's Tissue Transplant Program) under approval of the University of Texas Southwestern Institutional Review Board³². Brain tissue was collected at local medical examiners' offices after obtaining permissions. Blood toxicology was performed to exclude subjects using illicit drugs or psychotropic medications. Subjects with a known history of neurological disorders or head injury were also excluded. Demographic characteristics associated with each sample are listed in Supplementary Table 2. Clinical records and interviews were obtained for each case and reviewed by three or four mental health professionals to establish independent diagnoses followed by a consensus diagnosis in line with the Diagnostic and Statistical Manual of Mental Disorders (DSM) IV criteria. Cohorts were matched as closely as possible for gender, age, race, pH, post-mortem interval and RNA integrity number³².

Stereotaxic surgery and viral gene transfer. All surgeries were performed under aseptic conditions using anesthetic as described previously³². Mice were anesthetized with a mixture of ketamine/xylazine, as mentioned in the IHC section, and positioned in a small animal stereotaxic instrument (David Kopf Instruments). The skull surface was exposed and 30-gauge syringe needles (Hamilton Co.) were used to bilaterally infuse 0.5 μl of virus (1.0 × 10¹¹ infectious unit/mL) expressing either³³ AAV2/9-shRNA or AAV2/9-shRNA-Cldn5 into the NAc (bregma coordinates: anteroposterior +1.6 mm, mediolateral +1.5 mm, dorsoventral −4.4 mm) or hippocampus (bregma coordinates: anteroposterior −2.0 mm, mediolateral +1.0 mm, dorsoventral −2.2 mm) at a rate of 0.1 μL/min. All mice were allowed to recover for 2 weeks before activation of the viruses with doxycycline treatment (2 mg/mL in drinking water). Placement was validated with visualization of blood vessels with EB, green fluorescent protein (GFP) and Cldn5 IHC. Briefly, virus-injected mice were anesthetized and retro-orbital injection of EB was performed as described in the IHC section. Brains were collected after 10 min, fixed overnight, cryoprotected with 30% sucrose and frozen and 50-μm-thickness slices produced on a brain vibratome. After a quick wash in 0.1 M PBS, slices were transferred to blocking solution (2% NDS and 0.05% Triton X-100 in 0.1 M PBS) for 2 h before overnight incubation in primary antibody solution (anti-rabbit Cldn5, 1:250, Life Technologies, #34-1600; anti-chicken GFP, 1:1,000, Aves, #GFP-1020 in 2% NDS and 0.05% Triton X-100 in 0.1 M PBS). After three washes in 0.1 M PBS for 10 min, sections were incubated with anti-rabbit-Cy3 and anti-chicken-Cy2 secondary antibodies in 0.1 M PBS for 2 h (1:400, Jackson ImmunoResearch; #711-165-152 and #703-225-155), washed again three times with PBS and stained with DAPI. Slices were mounted and coverslipped with ProLong Diamond Antifade Mountant (Invitrogen).

Magnetic resonance imaging (MRI) scans. Following 10-d CSDS and SI behavioral screening, BBB permeability was analyzed using a small-rodent Bruker Biospec 7 T/30 scanner system located at the Translational and Molecular Imaging Institute (TMII) at Mount Sinai Hospital (details are included in the Life Sciences Reporting Summary). Mice were imaged under isoflurane anesthesia (5% in air for induction and 1.5% maintenance with 2 L/min flow rate). Baseline T1-weighted images were acquired using a FLASH sequence (32 slices, thickness 0.5 mm, in-plane resolution 78 mm × 78 mm). Gadolinium contrast agent Gd-DTPA was then administered through retro-orbital injection. The concentration was 0.3 mmol/kg and a bolus of 0.1 mL was injected. The animals were then rescanned using the same T1 protocol 25 min after injection. Images were analyzed using in-house software developed under Matlab V2015b (MathWorks Inc., Natick, MA). Regions of interest (ROIs) were manually defined on the images and mean image intensities were extracted. Signal enhancement was defined as (Post − Pre)/Post.

Detection of injected tracers. Tracers were administered through retro-orbital injection in anesthetized animals (mixture of ketamine/xylazine) following 10-d CSDS and SI test screening. Quantification of BBB-related dyes was performed using unbiased extraction assays as described previously⁵³ with slight modifications to apply the protocol to specific brain regions instead of the entire brain. Briefly, EB (Sigma, 2% wt/vol, 6 µl/g of body weight) was allowed to circulate for 10 min in unperfused animals used for IHC or for 16 h followed by 5 min intracardiac perfusion with 0.1 M PBS in mice used for comparative EB infiltration (IHC) and quantification. After perfusion the brain was removed and bilateral NAC, hippocampus and PFC punches were collected from 1-mm-thick coronal slices in 1.5-mL microcentrifuge tubes previously weighed. Microcentrifuge tubes containing samples were weighed again before adding 100 µl pure dimethylformamide to each tube. Extraction was performed at 55 °C for 72 h. The samples were centrifuged at 21,000 g for 30 min and the supernatant collected. EB fluorescence of each sample was obtained on a SpectraMax 340PC384 microplate reader (Molecular Devices) and calculated from a serial dilution fluorescence curve using SoftMax Pro 5.2 software. A kidney lysate was used as a positive control.

Similarly, cadaverine conjugated to Alexa Fluor 555 (Life Technologies) was administered through retro-orbital injection and allowed to circulate for 2 h in unstressed control and defeated mice. For quantification, anesthetized animals were perfused for 5 min with 0.1 M PBS and then bilateral NAC, hippocampus and PFC punches were collected in previously weighed microcentrifuge tubes for tracer extraction. Samples were weighed, homogenized in 1% Triton X-100 in 0.1 M PBS and centrifuged at 21,000 g for 20 min. Relative fluorescence of the supernatant was measured on a SpectraMax 340PC384 microplate reader (Molecular Devices) and calculated from a serial dilution fluorescence curve using SoftMax Pro 5.2 software.

Isolation of brain leukocytes and flow cytometry. Mice were deeply anesthetized with a lethal dose of chloral hydrate and transcardially perfused with 0.1 M PBS. Brain was removed and one forebrain hemisphere (without olfactory bulb) was minced, incubated in phenol-red-free DMEM supplemented with 2% heat inactivated FBS, 10 mM HEPES and collagenase type IV (0.4 mg/mL) for 15 min and then passed through a 19G blunt syringe to obtain a homogeneous cell suspension. Mononuclear cells were separated with a 40% Percoll gradient. Isolated cells were surface stained in FACS buffer for 20–30 min on ice with the following antibodies: CD11b (clone M1/70, eBioscience), F4/80 (clone CI: A3-1, Bio-Rad), CD45 (clone 30F11, eBioscience), MHC II (clone M5/114.15.2, eBioscience), CD3e (clone 145-2C11, Biolegend), Gr-1 (clone RB6-8C5, Biolegend), CD115 (clone AFS98, eBioscience). Multiparameter analysis was performed on a LSR II Fortessa (BD) and analyzed with FlowJo software (Tree Star) (details are included in the Life Sciences Reporting Summary). Dead cells and doublets were excluded from all analysis.

IL-6 biotinylation. Recombinant mouse IL-6 (RMIL6I, Thermo Fisher Scientific) was dissolved in 0.1 M sodium bicarbonate buffer, pH 7.5, and biotin-X SE (6-(biotinoyl)amino)hexanoic acid, succinimidyl ester (biotinamidocaproate, N-hydroxysuccinimidyl ester) in dimethylsulfoxide. Conjugation of biotin with IL-6 was performed at pH 7.5 with a 2:1 molar ratio, respectively, by slowly adding biotin to the vortexing protein solution followed by incubation for 60 min at room temperature with continuous agitation. Conjugated IL-6-biotin (~21.45 kDa) was separated from unbound biotin (~0.45 kDa) using high-performance size-exclusion chromatography resin Zeba Spin Desalting Columns, 7K MWCO, 0.5 mL (Thermo Fisher Scientific), which is characterized by 95% retention and removal of salts and other small molecules (< 1 kDa) and recovery of proteins and other macromolecules (> 7 kDa). The conjugate was diluted in saline solution to a final concentration of 20 µg/mL. Biotinylated IL-6 (20 ng diluted in saline solution) was administered through retro-orbital injection in CTRL, SS or RES mice 24 h after SI test screening and allowed to circulate for 2 h. The mice were then anesthetized with a mixture of ketamine and xylazine and perfused with 0.1 M PBS for 5 min. The brain was collected and fixed overnight in 4% PFA. Brains were cryoprotected with 30% sucrose, frozen and then sliced on the cryostat at a thickness of 40 µm. IL-6-biotin conjugate was detected with Oregon Green-488 conjugate of NeutrAvidin biotin-binding protein (Thermo Fisher Scientific), a form of avidin that has been processed to remove carbohydrate and lower its isoelectric point substantially, decreasing background due to nonspecific binding. Double labeling with the perivascular marker CD31 (rat anti-CD31, 1:150, BD Biosciences, #550274; anti-rat-Cy5, 1:400, Jackson ImmunoResearch, #5550274) was performed as described in the IHC section. After three washes with 0.1 M PBS, slices were stained with DAPI, mounted, and coverslipped with ProLong Diamond Antifade Mountant (Invitrogen).

IL-6 i.p. injection and ELISA. Stress-naïve mice were administered saline solution or 5 or 15 ng/mL mouse recombinant IL-6 diluted in saline solution through i.p. injection 20 min before tissue collection. Blood serum and bilateral NAC punches were collected in 1-mm-thick coronal sections on wet ice and IL-6 levels were

detected with a solid-phase sandwich IL-6 ELISA (BD Biosciences, #550950). IL-6 levels were measured on a SpectraMax 340PC384 microplate reader (Molecular Devices) and calculated from a serial dilution curve using SoftMax Pro 5.2 software. Another cohort of mice went through 10-d CSDS and SI behavioral screening before blood serum, NAC, hippocampus and PFC tissue collection and assessment of IL-6 levels by ELISA (R&D Systems, #SM6000B).

Osmotic minipump surgery and IL-6 infusion. Mice were anesthetized with a mixture of ketamine/xylazine as described in the previous sections and surgically implanted with bilateral NAC guide cannulae (Plastic One). Cannulae (Plastics One) were delivered into the NAC according to bregma coordinates (anteroposterior +1.6 mm, mediolateral +1.5 mm, dorsoventral -4.4 mm) and fixed to the skull with Loctite skull adhesive (Henkel). Saline or a total of 5 ng of IL-6 (diluted at 10 ng/mL in saline solution) was administered over 5 min (0.1 mL/min) using a mini-pump (Harvard Apparatus), followed by a 20-min rest, before the subthreshold microdefeat stress. SI test was conducted 24 h later. Mice were then sacrificed and perfused as described above in the IHC section to confirm placement of cannula in the NAC.

Statistical analysis. Sample size for CSDS mouse cohorts was calculated based on previous studies of CSDS and depression-like behaviors^{11,32} (details are included in the Life Sciences Reporting Summary). Outliers for social interaction (SI) test screening were identified as being greater than 2 s.d. from the mean and excluded. All mice were assigned to stress-susceptible (SS) or resilient (RES) groups on the basis of their behavioral profile when compared to unstressed controls (CTRL). CTRL and SS mice were randomly assigned to vehicle or imipramine treatment groups using the Excel spreadsheet random function. SI screening and behavioral tests were performed with automated tracking systems when possible. If not (for splash test, sucrose preference test and forced swim test), scoring was done by experimenters blinded to experimental conditions. Outliers for behavioral testing—for example, those characterized by impaired locomotion—were identified as being greater than 2 s.d. from the mean and excluded from statistical analysis. One unstressed AAV-shRNA-Cldn5 mouse was excluded after verification of virus injection placement. All *t*-tests, one-way ANOVAs, two-way ANOVAs and Pearson's correlations were performed using GraphPad Prism software (GraphPad Software Inc.). Statistical significance was set at $P < 0.05$. Bonferroni was used as a post hoc test when appropriate for one-way and two-way ANOVAs and statistical significance was set at $P < 0.05$. Detailed statistics are presented in the Supplementary Data. Visual representation of average and s.e.m. with heat maps was done using Matlab-based software. Individual values were used to compute correlation matrices and *P* values were determined by Matlab-based software. Normality was determined by Kolmogorov-Smirnov, D'Agostino-Pearson and Shapiro-Wilk normality tests using GraphPad Prism software. All quantitative PCR, immunohistochemistry and BBB-related tracer quantification were performed in duplicate in two different cohorts of mice.

Data availability. All data supporting the findings of this study are available within the paper and Supplementary Information files.

References

- Golden, S. A. et al. Basal forebrain projections to the lateral habenula modulate aggression reward. *Nature* **534**, 688–692 (2016).
- Mishra, V. et al. Primary blast causes mild, moderate, severe and lethal TBI with increasing blast overpressures: experimental rat injury model. *Sci. Rep.* **6**, 26992 (2016).
- Keaney, J. et al. Autoregulated paracellular clearance of amyloid-β across the blood-brain barrier. *Sci. Adv.* **1**, e1500472 (2015).
- Campbell, M. et al. RNAi-mediated reversible opening of the blood-brain barrier. *J. Gene Med.* **10**, 930–947 (2008).
- Doyle, S. L. et al. IL-18 attenuates experimental choroidal neovascularization as a potential therapy for wet age-related macular degeneration. *Sci. Transl. Med.* **6**, 230ra44 (2014).
- Wälchli, T. et al. Quantitative assessment of angiogenesis, perfused blood vessels and endothelial tip cells in the postnatal mouse brain. *Nat. Protoc.* **10**, 53–74 (2015).
- Blank, T. et al. Brain endothelial- and epithelial-specific interferon receptor chain 1 drives virus-induced sickness behavior and cognitive impairment. *Immunity* **44**, 901–912 (2016).
- Janssen, W. G. et al. Cellular and synaptic distribution of NR2A and NR2B in macaque monkey and rat hippocampus as visualized with subunit-specific monoclonal antibodies. *Exp. Neurol.* **191** (Suppl. 1), S28–S44 (2005).
- Armulik, A. et al. Pericytes regulate the blood-brain barrier. *Nature* **468**, 557–561 (2010).

Life Sciences Reporting Summary

Nature Research wishes to improve the reproducibility of the work that we publish. This form is intended for publication with all accepted life science papers and provides structure for consistency and transparency in reporting. Every life science submission will use this form; some list items might not apply to an individual manuscript, but all fields must be completed for clarity.

For further information on the points included in this form, see [Reporting Life Sciences Research](#). For further information on Nature Research policies, including our [data availability policy](#), see [Authors & Referees](#) and the [Editorial Policy Checklist](#).

▶ Experimental design

1. Sample size

Describe how sample size was determined.

Sample size for chronic social defeat stress (CSDS) mouse cohorts was calculated based on previous studies of CSDS and depression-like behaviors (Golden et al., 2013; Hodes et al., 2014).

2. Data exclusions

Describe any data exclusions.

Outliers for social interaction test screening were identified as being greater than two standard deviations from the mean and excluded. All mice were assigned to stress-susceptible (SS) or resilient (RES) groups based on their behavioral profile when compared to unstressed controls (CTRL). Outliers for behavioral testing, for example characterized by impaired locomotion, were identified as being greater than two standard deviations from the mean and excluded from statistical analysis. One unstressed AAV-shRNA-cldn5 mouse was excluded after verification of virus injection placement.

3. Replication

Describe whether the experimental findings were reliably reproduced.

Sample size for chronic social defeat stress (CSDS) mouse cohorts and behavioral experiments was calculated based on previous studies of CSDS and depression-like behaviors (Golden et al., 2013; Hodes et al., 2014). All quantitative PCR, immunohistochemistry and blood-brain barrier-related tracer quantification were performed in duplicate in two different cohorts of mice.

4. Randomization

Describe how samples/organisms/participants were allocated into experimental groups.

All mice were assigned to stress-susceptible (SS) or resilient (RES) groups based on their behavioral profile when compared to unstressed controls (CTRL). CTRL and SS mice were randomly assigned to vehicle or imipramine treatment groups using Excel spreadsheet random function.

5. Blinding

Describe whether the investigators were blinded to group allocation during data collection and/or analysis.

Social interaction test screening and behavioral tests were performed with automated tracking systems when possible. If not, scoring was done by experimenters blinded to experimental conditions (for splash test, sucrose preference test and forced swim test).

Note: all studies involving animals and/or human research participants must disclose whether blinding and randomization were used.

6. Statistical parameters

For all figures and tables that use statistical methods, confirm that the following items are present in relevant figure legends (or in the Methods section if additional space is needed).

- n/a Confirmed
- The exact sample size (n) for each experimental group/condition, given as a discrete number and unit of measurement (animals, litters, cultures, etc.)
 - A description of how samples were collected, noting whether measurements were taken from distinct samples or whether the same sample was measured repeatedly
 - A statement indicating how many times each experiment was replicated
 - The statistical test(s) used and whether they are one- or two-sided (note: only common tests should be described solely by name; more complex techniques should be described in the Methods section)
 - A description of any assumptions or corrections, such as an adjustment for multiple comparisons
 - The test results (e.g. P values) given as exact values whenever possible and with confidence intervals noted
 - A clear description of statistics including central tendency (e.g. median, mean) and variation (e.g. standard deviation, interquartile range)
 - Clearly defined error bars

See the web collection on [statistics for biologists](#) for further resources and guidance.

► Software

Policy information about [availability of computer code](#)

7. Software

Describe the software used to analyze the data in this study.

All t-tests, one-way ANOVAs, two-way ANOVAs and Pearson's correlations were performed using GraphPad Prism software (GraphPad Software Inc.). Statistical significance was set at $*p < 0.05$. Bonferroni was used as a post-hoc test when appropriate for one-way and two-way ANOVAs and statistical significance was set at $*p < 0.05$. Visual representation of average and SEM with heat maps was done using Matlab-based software. Individual values were used to compute correlation matrices and p values were determined by Matlab-based software. Normality was determined by Kolmogorov-Smirnov, D'Agostino-Pearson and Shapiro-Wilk normality tests using GraphPad Prism software.

For manuscripts utilizing custom algorithms or software that are central to the paper but not yet described in the published literature, software must be made available to editors and reviewers upon request. We strongly encourage code deposition in a community repository (e.g. GitHub). [Nature Methods guidance for providing algorithms and software for publication](#) provides further information on this topic.

► Materials and reagents

Policy information about [availability of materials](#)

8. Materials availability

Indicate whether there are restrictions on availability of unique materials or if these materials are only available for distribution by a for-profit company.

There is no restriction on availability of unique materials in this study.

9. Antibodies

Describe the antibodies used and how they were validated for use in the system under study (i.e. assay and species).

Primary antibodies were used according to the following conditions and references : rabbit anti-cldn5, 1:100, Life Technologies, #34-1600; rabbit anti-occludin, 1:250, Life Technologies, #40-4700; rabbit anti-ZO-1, 1:50; Life Technologies, #61-7300; anti-rat-CD31, 1:150, BD Biosciences, #5550274 (Campbell et al., 2008; Doyle et al., 2014; Keane et al., 2015).

10. Eukaryotic cell lines

- State the source of each eukaryotic cell line used.
- Describe the method of cell line authentication used.
- Report whether the cell lines were tested for mycoplasma contamination.
- If any of the cell lines used are listed in the database of commonly misidentified cell lines maintained by [ICLAC](#), provide a scientific rationale for their use.

Eukaryotic cell lines were not used in this study.

► Animals and human research participants

Policy information about [studies involving animals](#); when reporting animal research, follow the [ARRIVE guidelines](#)

11. Description of research animals

Provide details on animals and/or animal-derived materials used in the study.

Male C57BL/6J mice (about 25 g) were purchased at 7 weeks of age from the Jackson Laboratory and allowed one week of acclimation to the Icahn School of Medicine at Mount Sinai (ISMMS) house facilities before the start of experiments. ccr2RFP:: cx3cr1GFP mice were bred at the ISMMS facilities and used at 8-10 weeks of age. Sexually experienced retired male CD-1 breeders (about 40 g) of at least 4 months of age were purchased from Charles River Laboratories and used as aggressors. All mice were single housed following CSDS and maintained on a 12-h/12-h light/dark cycle throughout. Mice were provided with ad libitum access to water and food except during the novelty-suppressed feeding test. Behavioral assessments and tissue collection were performed into the dark phase. All mouse procedures were performed in accordance with the National Institutes of Health Guide for Care and Use of Laboratory Animals and the ISMMS Animal Care and Use Committee.

Policy information about [studies involving human research participants](#)

12. Description of human research participants

Describe the covariate-relevant population characteristics of the human research participants.

Whole-tissue NAc, HIPp or PFC (BA25) resections were collected and provided by the Quebec Suicide Brain Bank at the Douglas Hospital Research Center (McGill University) under approval of the institution Ethics Committee for the Montreal cohort. For the Texas cohort, whole-tissue NAc resections were collected and provided by the Dallas Brain Collection (tissue was collected by the Dallas Medical Examiner's Office and the University of Texas Southwestern's Tissue Transplant Program) under approval of the University of Texas Southwestern Institutional Review Board. Brain tissue was collected at local medical examiners offices after obtaining permissions. Blood toxicology was performed to exclude subjects using illicit drugs or psychotropic medications. Subjects with knock history of neurological disorders or head injury were also excluded. Demographic characteristics associated with each sample are listed in Supplementary Information Table 2. Clinical records and interviews were obtained for each case and reviewed by three to four mental health professionals to establish independent diagnoses followed by a consensus diagnosis in line with the Diagnostic and Statistical Manual of Mental Disorders (DSM) IV criteria. Cohorts were matched as closely as possible for gender, age, race, pH, postmortem interval and RNA integrity number.

Flow Cytometry Reporting Summary

Form fields will expand as needed. Please do not leave fields blank.

▶ Data presentation

For all flow cytometry data, confirm that:

- 1. The axis labels state the marker and fluorochrome used (e.g. CD4-FITC).
- 2. The axis scales are clearly visible. Include numbers along axes only for bottom left plot of group (a 'group' is an analysis of identical markers).
- 3. All plots are contour plots with outliers or pseudocolor plots.
- 4. A numerical value for number of cells or percentage (with statistics) is provided.

▶ Methodological details

5. Describe the sample preparation.

Blood was collected by submandibular vein bleed into EDTA-lined tubes (Sarstedt) 100 uL blood was transferred into FACS buffer (PBS w/o Ca²⁺ Mg²⁺ supplemented with 2% heat inactivated FBS and 5mM EDTA), and red blood cells (RBC) were lysed in 1× RBC Lysis solution (eBioscience). For brain leukocyte isolation, mice were deeply anesthetized with a lethal dose of choral hydrate and transcardially perfused with PBS. Brain was removed and one forebrain hemisphere (without olfactory bulb) was minced, incubated in phenol-red free DMEM supplemented with 2% heat inactivated FBS, 10mM HEPES and Collagenase type IV (0.4 mg/mL) for 15 min and then passed through a 19G blunt syringe to obtain a homogeneous cell suspension. Mononuclear cells were separated with a 40% Percoll gradient. Isolated cells were surface stained in FACS buffer for 20-30 min on ice with the following antibodies: CD11b (clone M1/70, eBioscience), F4/80 (clone CI: A3-1, BioRad), CD45 (clone 30F11, eBioscience), MHC II (clone M5/114.15.2, eBioscience), CD3e (clone 145-2C11, Biolegend), Gr-1 (clone RB6-8C5, Biolegend), CD115 (clone AFS98, eBioscience).

6. Identify the instrument used for data collection.

BD LSR II Fortessa

7. Describe the software used to collect and analyze the flow cytometry data.

Data were collected using BD FACSDiva software and analyzed with FlowJo software (Tree Star).

8. Describe the abundance of the relevant cell populations within post-sort fractions.

Post-sort fractions were not used in this study.

9. Describe the gating strategy used.

ccr2RFP+ monocytes were gated as single, live, CD11b+ F4/80+ ccr2RFP+ cx3cr1GFP-. cx3cr1GFP+ microglia were gated as single, live, CD11b+ F4/80+ ccr2RFP- cx3cr1GFP+.

Tick this box to confirm that a figure exemplifying the gating strategy is provided in the Supplementary Information.

MRI Studies Reporting Summary

Form fields will expand as needed. Please do not leave fields blank.

▶ Experimental design

1. Describe the experimental design.

Gd-DTPA perfusion scan were compared to baseline scans. The mice received a baseline scan followed by an injection of Gd-DTPA (.3mmol/kg) with a volume of 0.1ml. The Repeat scan was obtained 25 mins after injection as described in the Material and Methods section, page 34.
2. Specify the number of blocks, trials or experimental units per session and/or subject, and specify the length of each trial or block (if trials are blocked) and interval between trials.

Each mouse was scanned once 25 mins after Gd-DTPA injection for 15 minutes.
3. Describe how behavioral performance was measured.

Behavioral phenotype of stressed mice was performed using the social interaction test. All mice were assigned to stress-susceptible (SS) or resilient (RES) groups based on their behavioral profile when compared to unstressed controls (CTRL).

▶ Acquisition

4. Imaging
 - a. Specify the type(s) of imaging.

T1
 - b. Specify the field strength (in Tesla).

7 Tesla
 - c. Provide the essential sequence imaging parameters.

FLASH sequence, TE=4ms, TR=304ms, 4 Averages, Flip angle=75 degrees. FOV=20mm, 256x256, Slice thickness=0.5mm, 32 slices
 - d. For diffusion MRI, provide full details of imaging parameters.

No diffusion was acquired
5. State area of acquisition.

New York

▶ Preprocessing

6. Describe the software used for preprocessing.

Post injection images were reconstructed using the same scaling factor (gain) as the pre-injection scan. Subsequently an in-house script was used to convert from Raw Bruker format to Nifti format. In-house software based on Matlab V2013 (Mathworks Inc, Natick, MA) was used to extract Region of Interests (ROI) from the images.
7. Normalization
 - a. If data were normalized/standardized, describe the approach(es).

Data were not normalized in this study.
 - b. Describe the template used for normalization/transformation.

Data were not normalized/transformed in this study.
8. Describe your procedure for artifact and structured noise removal.

No artifact of structured noised was removed in this study.

9. Define your software and/or method and criteria for volume censoring, and state the extent of such censoring.

No volume censoring was performed in this study.

► Statistical modeling & inference

10. Define your model type and settings.

Series of ROI mean values were normalized to the unstressed control group average and compared for each brain region.

11. Specify the precise effect tested.

ROI values were compared for each brain region using one-way ANOVA and Bonferroni's Multiple Comparison Test. Correlation between individual ROI values and social interaction ratio was evaluated using Pearson's test.

12. Analysis

- a. Specify whether analysis is whole brain or ROI-based.

ROI means were obtained for the bilateral Prefrontal cortex, Nucleus Accumbens, Striatum, Hippocampus, Thalamus, Somatosensory Cortex, Insular Cortex

- b. If ROI-based, describe how anatomical locations were determined.

ROI positions were visually identified

13. State the statistic type for inference.
(See [Eklund et al. 2016](#).)

No inference was applied in this study.

14. Describe the type of correction and how it is obtained for multiple comparisons.

No correction was applied in this study.

15. Connectivity

- a. For functional and/or effective connectivity, report the measures of dependence used and the model details.

No functional and/or effective connectivity measures were included in this study.

- b. For graph analysis, report the dependent variable and functional connectivity measure.

No functional and/or effective connectivity measures were included in this study.

16. For multivariate modeling and predictive analysis, specify independent variables, features extraction and dimension reduction, model, training and evaluation metrics.

No modeling or predictive analysis was included in this study.